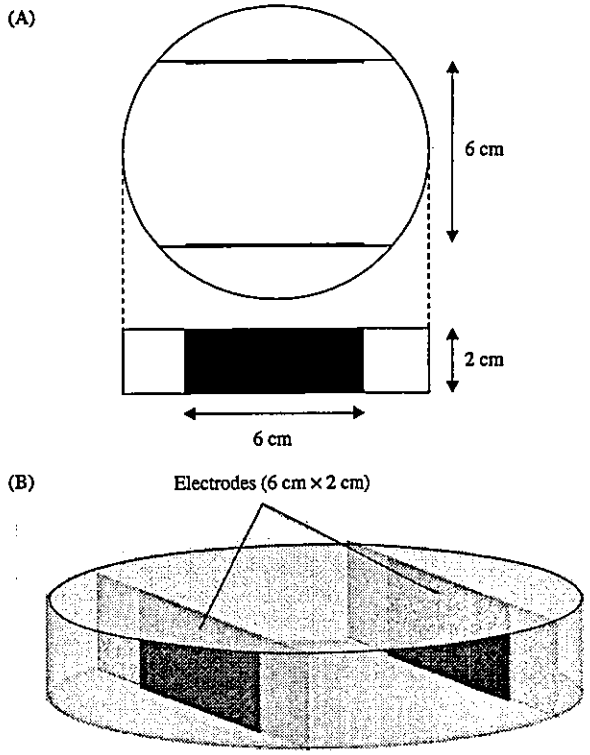

Figure 2. Electroporator. Plane and side view (A) and a schematic illustration (B). Electrodes are parallel (6 × 2 cm stainless steel) and fixed on glass slides. Inter-electrode distance: 6 cm

electroporation, we rechecked the actual electric current and voltage.

Plasmid DNA

pCAGGS-luc and *pCAGGS-EGFP* plasmids were constructed by cloning the luciferase and enhanced green fluorescent protein (EGFP) cDNAs, respectively, into *pCAGGS* [8,11]. *pCAGGS* contains a CMV enhancer and beta-actin promoter and was kindly provided by Drs. Isaka and Yamato (Osaka University Graduate School of Medicine, Osaka, Japan). Plasmids were grown in *Escherichia coli* strain DH5α and extracted by a Concert™ high-purity plasmid Maxiprep system (Gibco™, Invitrogen Corporation). DNA was dissolved in TE buffer and plasmid solution (1 mg/ml) was stored at −20 °C before use. The quantity and quality of DNA were assessed by measuring the optical density at 260 and 280 nm. We used 100 μg/ml plasmid solution, which was diluted with TE buffer or one of several different osmotic pressure solutions (20, 110, 200, 290 and 310 mOsm/kg) before use in all experiments.

Luciferase assay

The protocol used to process tissue homogenates for the luciferase assay system was similar to that described previously [13]. Briefly, the transfected liver lobe was dissected out under anesthesia, cut into small pieces, and stored at −80 °C until luciferase assay. Liver tissue was treated with 0.7 ml of 1 × luciferase cell culture lysis buffer (Promega, Tokyo, Japan), re-stored at −80 °C, and centrifuged at 12 000 rpm for 2 min at 4 °C after dissolution. The lysate supernatant was used for the luciferase assay and determination of protein concentration. Luciferase activity was measured using the luciferase assay system (Promega) in a luminometer (Lumat LB9501; Berthold, Wildbad, Germany). Enzyme activity was expressed relative to liver protein concentration, which was determined using the Bio-Rad protein assay system (Bio-Rad, Hercules, CA, USA) [14]. Data are expressed as corrected luciferase activity (luciferase activity/protein concentration) for each individual transfected liver. Experiments were repeated at least three times.

Gene transfer in different conditions

Four rats in each group were examined for liver luciferase activity, several days after transfection. Firstly, rats were sacrificed on day 1 after gene transfer using different electroporator solutions at the same voltage and almost identical actual electric currents for gene transfer. Cold preservation solutions for transplantation, such as lactated Ringer's (LR) solution, University of Wisconsin (UW) solution, and histidine-tryptophan-ketoglutarate (HTK) solution, were used as electroporator solutions. Secondly, rats were sacrificed on day 1 after gene transfer using HTK solution as the electroporator solution at several different voltages. Thirdly, rats were sacrificed on day 1 after gene transfer following 400-V electroporation in HTK solution, combined with injection of 1 ml of *pCAGGS-luc* (100 μg/ml), which was diluted with one of several saline solutions of different osmotic pressure. Fourthly, rats were sacrificed on days 1, 3, 7 or 14 after gene transfer following 400-V electroporation in HTK solution combined with injection of 1 ml of *pCAGGS-luc* (100 μg/ml), to assess the time-course of luciferase activity. Finally, we determined the gene expression in the left lobe of the transplanted liver, small intestine, pre-tibial muscle, kidney, heart, lung, brain, and bone marrow, 1 day after injection of 1 ml of *pCAGGS-luc* (100 μg/ml) into the right and caudal lobe via the portal vein under electrical pulses of 400 V, to assess the gene expression at distant sites.

Measurement of liver enzymes

Blood was extracted from the abdominal aorta at the time of sacrifice, and plasma was obtained by centrifugation with 0.12–0.15% EDTA-2Na (1500 *g*, 10 min). The serum alanine aminotransferase (ALT) concentration was assayed using an automated blood analyzer (SPOT CHEM™, Arkray).

Measurement of osmotic pressure

We measured the osmotic pressure of plasmid solutions, which were diluted with solutions of saline (20 and 290 mOsm/kg) using an automated osmotic pressure analyzer (OSMOSTATION™(OM-0605), Arkray).

Fluorescence microscopy of EGFP

To identify cells expressing the transferred gene, we examined frozen sections of the liver lobe injected with enhanced green fluorescent protein (EGFP) by fluorescence microscopy. We analyzed the transfected right and caudal lobes of livers obtained from four rats in each group, 1 day after 400-V electroporation in HTK solution combined with injection of 1 ml of EGFP plasmid (100 μg/ml); *pCAGGS*-transfected liver was used as control. Transfected lobes were immediately resected, embedded in OCT compound and frozen in liquid nitrogen for fluorescence microscopy. Serial sections (8 μm) were cut with a cryostat and placed on slide glasses, and examined by fluorescence microscopy. Images were captured by a color cool charged-couple device camera (VB-6000; Keyence Co. Ltd., Osaka, Japan). All images were exposed using the same exposure time under the same magnification.

Statistical analysis

Data are expressed as mean ± standard deviation. Statistical analysis was performed using Statview J software (version 5.0). Student's *t*-test and one-way ANOVA were used for comparisons of luciferase activity, and Spearman's rank correlation coefficient was used to examine the correlation between various gene transfer conditions and luciferase activity. A P value of less than 0.05 denoted the presence of a statistically significant difference.

Results

Effects of the electrical resistance of electroporator solution on gene expression

To investigate the influence of electrical resistance of the electroporator solution and graft liver, we examined the efficacy of gene transfer with the luciferase reporter gene, *pCAGGS-luc*, using several cold preservation solutions as the electroporator solutions, at the same actual voltage and almost identical actual electric currents. We first assessed gene transfer efficacy using LR, UW, and HTK solutions at the same voltage (150 V). We also assessed gene transfer efficacy with injected plasmid solution, but without electroporation, as control. Differences between the preselected and the actual voltages were less than 2 V. The actual electric currents for electroporation were 1.65 ± 0.09, 1.05 ± 0.05, and 0.69 ± 0.13 A, respectively ($P < 0.05$). We then analyzed the relationship between luciferase activity and the actual electric current. For the actual electric current (OA), we examined transfected lobes of the liver graft, which were injected with *pCAGGS-luc* plasmid solution but not electroporated. Luciferase activities increased with elevation of the actual electric current, and the differences were statistically significant (Figure 3A, $P < 0.05$). Luciferase activity correlated with the actual electric current at the same actual voltage (luciferase activity vs. electric current, $r^2 = 0.379$, $P < 0.05$).

Next, we examined gene transfer efficacy using different cold preservation solutions at almost the same electric current (1.40–1.70 A). Initially, we determined the voltage that would give almost the same electric current. When the preselected voltages were 150 V in LR, 250 V in UW, and 350 V in HTK, the actual electric currents were 1.65 ± 0.09, 1.57 ± 0.19, and 1.41 ± 0.03 A, respectively ($P = 0.21$). The differences between the preselected voltages and the actual voltages were less than 2 V. Next,

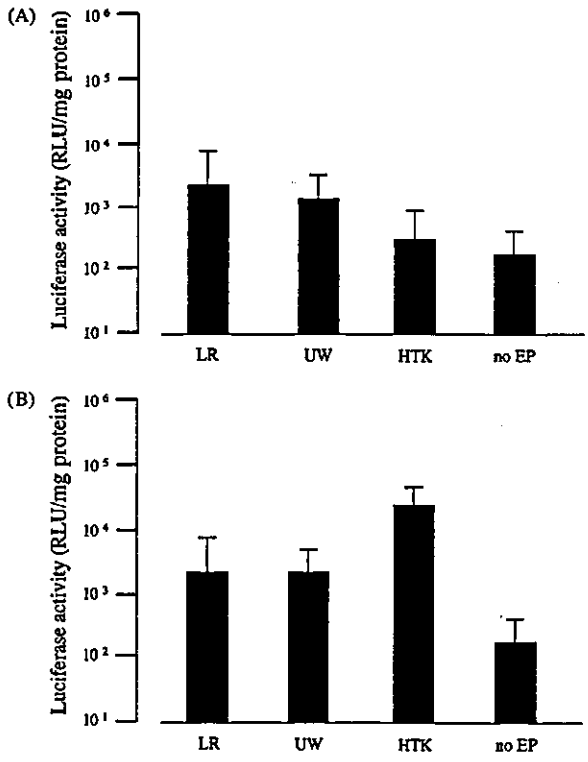

Figure 3. Effect of electroporator solution on luciferase activity. Liver specimens were obtained on day 1 after *pCAGGS-luc* plasmid transfer combined with electroporation. (A) Luciferase activity with various electroporation solutions at the same preselected voltage (150 V). (B) Luciferase activity at various electroporation solutions at almost identical electrical currents (1.40–1.70 A). Each value represents the mean luciferase activity ± SD of four rats. LR, Lactated Ringer's solution; UW, University of Wisconsin solution; HTK, histidine-tryptophan-ketoglutarate solution; no EP, the liver graft was not electroporated

we examined luciferase activities at these preselected voltages. At the actual voltage (0 V), we examined transfected lobes of the liver graft that were injected with *pCAGGS-luc* plasmid solution but not electroporated. Luciferase activity also increased with elevation of the actual voltage and the differences were statistically significant (Figure 3B, $P < 0.05$). We also analyzed the relationship between luciferase activity and actual voltage. Luciferase activity correlated with actual voltage when the actual electric current was almost identical (luciferase activity vs. voltage, $r^2 = 0.350$, $P < 0.05$).

To confirm voltage dependency in the same electroporation solution, we examined gene transfer efficacy in HTK electroporation solution at 150, 250, 350 and 450 V. For the actual voltage (0 V), we examined transfected lobes of the liver graft that were injected with *pCAGGS-luc* plasmid solution but not electroporated. Although the differences between the preselected voltage and the actual voltage were less than 2 V at 150, 250 and 350 V, the actual voltage for the preselected voltage of 450 V was 372 ± 63 V (to the limit of the pulse generator). The actual electric currents were 0.69 ± 0.13, 1.16 ± 0.06, 1.41 ± 0.03, and 1.40 ± 0.05 A, respectively ($P < 0.05$). Luciferase activity increased with elevation of the actual voltage and the differences were statistically significant (Figure 4, $P = 0.0013$). There were no significant differences between luciferase activities at the preselected voltages of 350 and 450 V ($P = 0.63$). We also analyzed the relationship between luciferase activity and actual voltage. Luciferase activity correlated with actual voltage between preselected voltages of 0 and 350 V (luciferase activity vs. voltage, $r^2 = 0.469$, $P < 0.05$).

Effect of plasmid solution osmotic pressure on gene expression

We examined the efficacy of gene transfer using plasmid solutions of several osmotic pressures which were injected at the same voltage. Prior to injection, preserved plasmid solution (1 mg/ml) was added, along with 900 µl of one of several osmotic pressure saline solutions (20, 110, 200, 290 and 310 mOsm/kg). The actual osmotic pressures were 85 ± 2 and 325 ± 3 mOsm/kg in the solutions, which were diluted with 20 and 290 mOsm/kg solution of salt, respectively. Luciferase activity decreased with increasing plasmid solution osmotic pressure (Figure 5, $P < 0.05$). We also analyzed the relationship between luciferase activity and osmotic pressure of the added salt solution and found that luciferase activity correlated with osmotic pressure (luciferase activity vs. osmotic pressure, $r^2 = 0.466$, $P < 0.05$). Liver damage caused by electroporation and hypotonic plasmid solutions was assessed by elevation of serum ALT. ALT levels were 1131 ± 834 U/l in 20 mOsm/kg, 1007 ± 294 U/l in 110 mOsm/kg, 502 ± 288 U/l in 200 mOsm/kg, and 471 ± 246 U/l in 290 mOsm/kg, ($P = 0.17$). We compared gene transfer efficacy and liver damage between rats in which the liver graft was 400-V electroporated in HTK solution and rats that were not electroporated. Luciferase activities were higher at 400-V electroporation than without electroporation (Figure 5, $P < 0.05$). ALT levels were 1131 ± 834 U/l after 400-V electroporation and 1034 ± 127 U/l with no electroporation ($P = 0.825$).

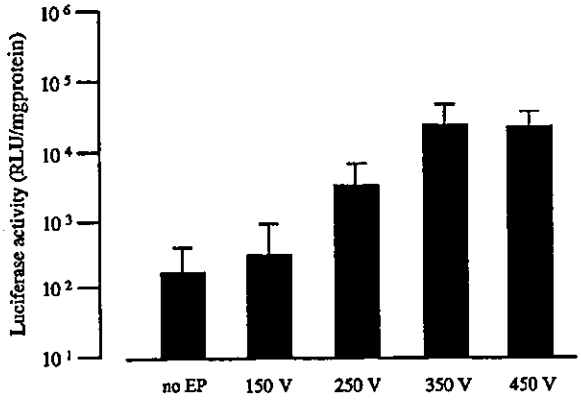

Figure 4. Effect of electric voltage in the same electroporator solution on luciferase activity. Luciferase activities were measured in liver specimens that were obtained on day 1 after *pCAGGS-luc* plasmid transfer combined with electroporation at various electrical voltages in HTK solution. Each value represents the mean luciferase activity ± SD of four rats. no EP, the liver graft was not electroporated

Time-course of luciferase activity

We also evaluated the time-course of changes in luciferase activity following direct gene transfer into the liver via *ex vivo* electroporation on days 1, 3, 7 and 14. In these experiments, 1 ml of *pCAGGS-luc* (100 µg/ml) was injected into the right and caudal lobes, and electroporated in HTK solution at 400 V. Luciferase activity was highest on day 1, and decreased gradually with time thereafter (Figure 6). On day 14, the luciferase activity was not statistically different from the activity without electroporation.

Luciferase activity in other organs

We confirmed the lack of gene expression in organs apart from the target sites in the right and caudal lobes. 1.0 ml of *pCAGGS-luc* plasmid (100 µg/ml) was injected into the right and caudal lobes of the liver graft via the portal vein, with electroporation at 400 V applied in HTK solution. Luciferase activity was estimated on day 1 in the lobe into which the plasmid was injected, and also in the non-injected lobe, small intestine, pre-tibial muscle, kidney, heart, lung, brain and bone marrow. Luciferase activities in organs other than the liver were less than 100 RLU/mg protein and <0.1% of that in the injected lobe ($P < 0.05$). In the non-injected liver lobe, luciferase activity was also less than 100 RLU/mg protein and <0.1% of that in the injected lobe ($P < 0.05$).

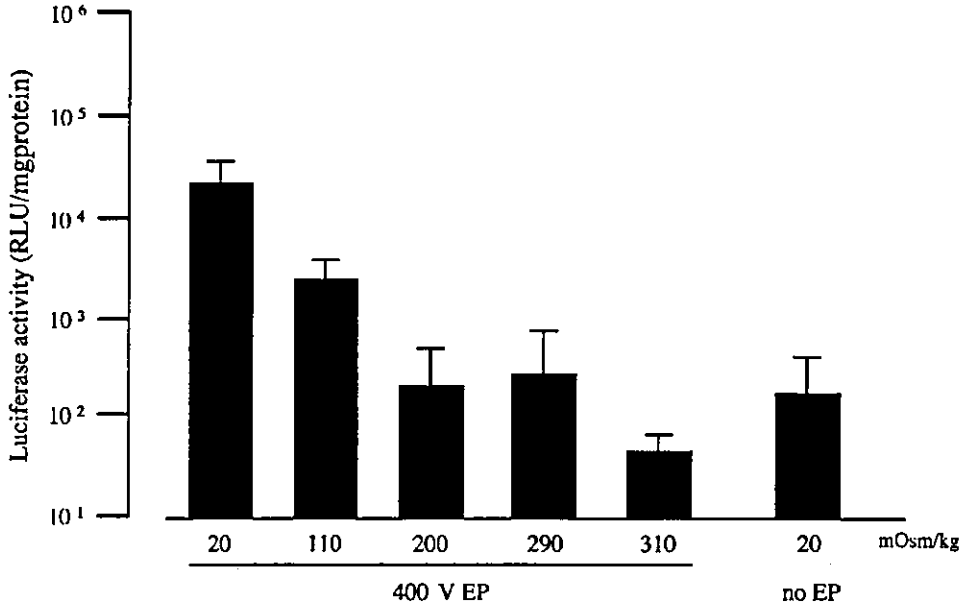

Figure 5. Effect of plasmid solution osmotic pressure on luciferase activity. Luciferase activities were measured in liver specimens that were obtained on day 1 after *pCAGGS-luc* plasmid transfer combined with electroporation and injection of various osmotic pressure plasmid solutions in the same electroporation solution (HTK solution) and voltage (400 V). Each value represents the mean luciferase activity ± SD of four rats. EP, the liver graft was electroporated; no EP, the liver graft was not electroporated

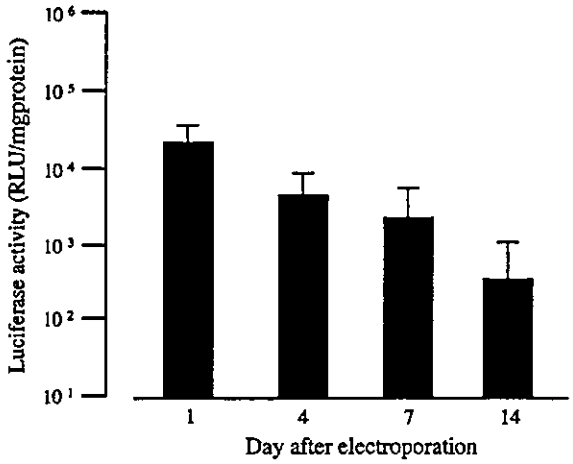

Figure 6. Time-course of luciferase activity after transfer of *pCAGGS-luc* by *ex vivo* electroporation. The *pCAGGS-luc* plasmid (1.0 ml, 100 μg/ml) was injected into the caudal and right lobes of the liver, and an electric pulse of 400 V was delivered in HTK solution. Each value represents the mean luciferase activity ± SD of four rats

EGFP expression in the liver after direct electroporation

To confirm gene expression after transfer, we used the *pCAGGS-EGFP* plasmid as a positive control and the *pCAGGS* plasmid as a negative control (Figure 7). No EGFP expression was noted in the negative control (Figure 7, left), whereas EGFP expression was detected in the positive control, particularly in perivascular cells, including hepatocytes (Figure 7, right).

Discussion

In this study, we successfully performed *ex vivo* electroporation-mediated gene transfer to a liver graft. Compared with electroporation-mediated gene transfer by forceps [8–10], clips [6], or needles [7], using our electroporator we could administer an electric field to the entire liver graft during the cold ischemia period. However, two extra conditions were considered in determining the optimal conditions for this procedure.

Firstly, the liver has a higher electrical resistance than the electroporation field. For *ex vivo* electroporation, the distance between the electrodes was a maximum of 1 cm, and we could achieve a sufficiently high electrical voltage to transduce plasmid in the liver. Several groups have reported the dependence of transfection efficacy on intensity of the electrical field [8,10,15,16], and higher voltages were required according to the thickness of target organ. In the present study, to achieve diffuse transduction of the plasmid in the liver graft, we constructed a dish-type electroporator, similar to an *in vitro* cell electroporator or *in vivo* embryo electroporator. It comprised 2 × 6 cm stainless steel electrodes with an inter-electrode distance of 6 cm. The electroporator was filled with LR, UW or HTK solution prior to electroporation, solutions selected from representative perfusion solutions for cold preservation. In contrast to *in vivo* electroporation using forceps, this technique will cause loss of electrical voltage to the liver, but provide an electrical field to the entire liver graft. Our present findings indicated that the electrical resistance of the electroporation solutions was, in increasing order, LR, UW, and HTK. We examined the transfection efficacy under conditions of equal electric current, voltage and

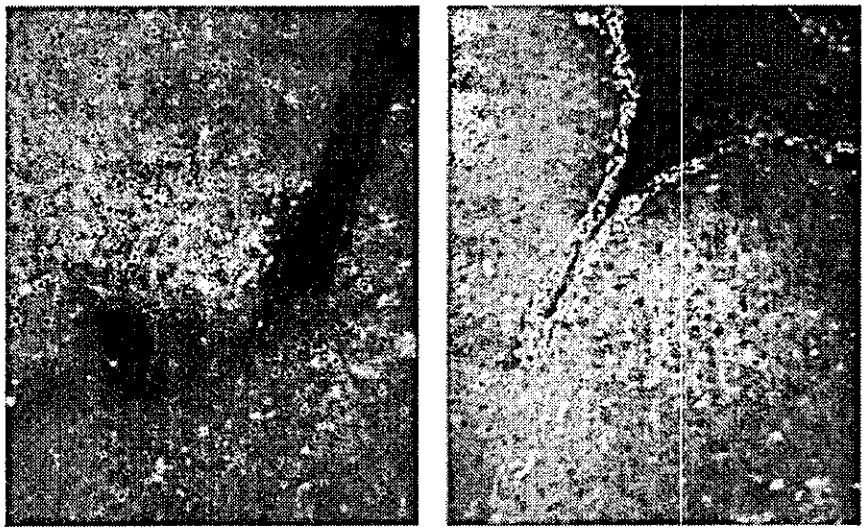

Figure 7. Representative microscopic findings after *EGFP* gene transfer by electroporation. Frozen sections (8-μm thick) were examined by fluorescence microscopy (×100). Liver specimens were resected 1 day after *pCAGGS-EGFP* transfection (right) and *pCAGGS* (left) transfection (control)

resistance, using the different electroporation solutions. Transfection efficacy was dependent on the intensity of the voltage at the same electric current, and, inversely, on the intensity of electric current at the same voltage. This finding seemed to invoke two phenomena, as follows: (1) The dependency of transfection efficacy on intensity of the electric field in the dish-type electroporator, similar to direct administration of electrical pulses via forceps, clips, and needles. We confirmed dependency on the intensity of the electrical field in the same electroporation solution. (2) The relationship between electrical resistance of the electroporation solution and transfection efficacy. There were differences in electric current and transfection efficacy at equal voltages in different electroporation solutions, indicating that the electroporation solution affected transfection efficacy. The transfection efficacy was higher in HTK solution, which has a higher electrical resistance for actual electric current at the same voltage than the other solutions. Although the transfection efficacy is dependent on intensity of the electric field, a low electrical resistance electroporation solution would cause loss of intensity, and thus higher electrical intensity is necessary for plasmid transduction, but would be dangerous due to the high electrical current required. In contrast, the electric pulse would be effective in the liver graft in high resistance electroporation solutions. Thus, high electrical resistance electroporation solutions appear to be advantageous for transfection efficacy.

Electroporation-mediated gene transfer requires a pressure gradient [4]. Several groups have reported that it was necessary to clamp the efferent vessel during electroporation [4,9], and others reported that they created local high-pressure conditions by direct plasmid injection to the target organ [6–8,15,17]. Previously, we reported the independence of transfection efficacy on injection pressure using TE buffer as a plasmid solution [10]. Furthermore, Liu *et al.* reported *in vivo* gene transfer to the liver in mice using electorporation following systemic administration of plasmid [18]. During transplantation, especially in living-donor liver transplantation, sufficiently long efferent vessels are not always available to facilitate their clamping for donor safety, and we could not apply pressure to the graft during the plasmid injection. We were able to transfect the plasmid into the liver in TE buffer, which is a low osmotic pressure solution, without injection pressure [10]. We prepared several plasmid solutions of various osmotic pressures, using salt, and found that under "no pressure" conditions, transfection efficacy was dependent on osmotic pressure. Transfection efficacy was very low in iso- or hypertonic plasmid solutions. We also confirmed this phenomenon using sucrose as an uncharged agent. Luciferase activities were 243 ± 386 in saline and 327 ± 270 in 245 mOsm sucrose, respectively (data not shown). Compared with the group that had plasmid injection into the graft without an electric pulse, the transfection efficacy was almost the same in isotonic plasmid solution and was lower in hypertonic plasmid solution. To date, no reports have directly discussed the relationship between transfection efficacy and osmotic pressure; however, our results lead us to speculate as follows. When an electrical pulse increases cell membrane permeability [19–21], plasmids migrate into the cytoplasm with plasmid solution when using a hypotonic solution. Elevations of liver transaminase (ALT) support this notion, because ALT levels were higher at lower osmotic pressure. Migration of the plasmid solution with the plasmid during electroporation probably causes cell expansion, resulting in elevated ALT levels. This cell expansion phenomenon is often observed during *in vivo* electroporation, and is thought to be due to colloid osmotic pressure [22–24]. Golzio *et al.* attempted

to prevent cell expansion by controlling colloid osmotic pressure using sucrose *in vitro* [20]. The size of the pores in the cell membrane after electroporation was estimated to be a maximum of approximately 10 nm [25], and transfer mechanisms of DNA and other particles seemed to differ [26]. These reports indicated that using particles other than DNA to maintain colloid osmotic pressure would decrease cell expansion and cell damage. For the *ex vivo* electroporation-mediated gene transfer described here, there are many factors impacting on transfection efficacy and graft damage, and this hypothesis would need to be tested.

Ex vivo gene transfer has another merit, which is the accuracy of controlling the gene expression site. The electric field is restricted to the graft after plasmid injection, so that gene expression would not be anticipated in other organs. We examined gene expression in other organs by luciferase assay 1 day after gene transfer. Luciferase activity was <0.1% of that in the liver graft and almost the same as background. Furthermore, we controlled gene expression in the liver graft. Compared with the plasmid-injected liver lobes (right and caudal lobes), luciferase activity was lower in the non-injected liver lobes (left and middle lobes). Under optimal conditions, we could transfer the gene into selective lobes of the liver graft. Gene expression in the graft was detected especially in the cells in perivascular areas, including hepatocytes. In previous reports, transduced cells were scattered throughout the liver after direct liver puncture with electroporation or naked plasmid DNA injection through afferent vessels with clamping of afferent and efferent vessels [4,17]. This difference in expression sites within the liver appears to reflect differences in local plasmid injection pressures. In previous studies, plasmids have been injected under pressure into the liver, whereas we did not apply any pressure to the liver graft during gene transfer. During pressure-mediated gene transfer, plasmids migrate to the interstitial spaces around hepatocytes due to the pressure, which causes the scattered distribution of expression in the liver. In the method we have described here, which was not mediated by injection pressure, gene expression was limited to a perivascular distribution, especially in endothelial cells. A comprehensive discussion of the benefits of these transfection models would require comparison of actual transfection efficacies using a range of other genes, for example, interleukins and growth factors.

In conclusion, we successfully performed *ex vivo* gene transfer into liver graft without requiring injection pressure, using a non-viral method, which resulted in reporter gene expression that was predominant in perivascular cells.

References

1. Shaked A, Csete ME, Shiraishi M, *et al.* Retroviral-mediated gene transfer into rat experimental liver transplant. *Transplantation* 1994; 57: 32–34.
2. Shaked A, Csete ME, Drazan KE, *et al.* Adenovirus-mediated gene transfer in the transplant setting. II. Successful expression of transferred cDNA in syngeneic liver grafts. *Transplantation* 1994; 57: 1508–1511.
3. Muruve DA, Barnes MJ, Stillman IE, *et al.* Adenoviral gene therapy leads to rapid induction of multiple chemokines and acute neutrophil-dependent hepatic injury in vivo. *Hum Gene Ther* 1999; 10: 965–976.
4. Zhang G, Vargo D, Budker V, *et al.* Expression of naked plasmid DNA injected into the afferent and efferent vessels of rodent and dog livers. *Hum Gene Ther* 1997; 8: 1763–1772.
5. Liu F, Song Y, Liu D. Hydrodynamics-based transfection in animals by systemic administration of plasmid DNA. *Gene Ther* 1999; 6: 1258–1266.
6. Titomirov AV, Sukharev S, Kistanova E. In vivo electroporation and stable transformation of skin cells of newborn mice by plasmid DNA. *Biochim Biophys Acta* 1991; 1088: 131–134.
7. Heller R, Jaroszeski M, Atkin A, *et al.* In vivo gene electroinjection and expression in rat liver. *FEBS Lett* 1996; 389: 225–228.
8. Aihara H, Miyazaki J. Gene transfer into muscle by electroporation in vivo. *Nat Biotechnol* 1998; 16: 867–870.
9. Tsujie M, Isaka Y, Nakamura H, *et al.* Electroporation-mediated gene transfer that targets glomeruli. *J Am Soc Nephrol* 2001; 12: 949–954.
10. Kobayashi S, Dono K, Tanaka T, *et al.* Gene transfer into the liver by plasmid injection into the portal vein combined with electroporation. *J Gene Med* 2003; 5: in press.
11. Kamada N, Calne RY. Orthotopic liver transplantation in the rat. Technique using cuff for portal vein anastomosis and biliary drainage. *Transplantation* 1979; 28: 47–50.
12. Hasuike Y, Monden M, Valdivia LA, *et al.* A simple method for orthotopic liver transplantation with arterial reconstruction in rats. *Transplantation* 1988; 45: 830–832.
13. Manthorpe M, Cornefert-Jensen F, Hartikka J, *et al.* Gene therapy by intramuscular injection of plasmid DNA: studies on firefly luciferase gene expression in mice. *Hum Gene Ther* 1993; 4: 419.
14. Schleicher E, Wieland OH. Evaluation of the Bradford method for protein determination in body fluids. *J Clin Chem Clin Biochem* 1978; 16: 533–534.
15. Heller L, Jaroszeski MJ, Coppola D, *et al.* Electrically mediated plasmid DNA delivery to hepatocellular carcinomas in vivo. *Gene Ther* 2000; 7: 826–829.
16. Bureau MF, Gehl J, Deleuze V, *et al.* Importance of association between permeabilization and electrophoretic forces for intramuscular DNA electrotransfer. *Biochim Biophys Acta* 2000; 1474: 353–359.
17. Suzuki T, Shin BC, Fujikura K, *et al.* Direct gene transfer into rat liver cells by in vivo electroporation. *FEBS Lett* 1998; 425: 436–440.
18. Liu F, Haung L. Electric gene transfer to the liver following systemic administration of plasmid DNA. *Gene Ther* 2002; 9: 1116–1119.
19. Chang DG, Chassy BM, Saunders JA, *et al.* *Guide for Electroporation and Electrofusion*, Academic Press: San Diego, 1992.
20. Golzio M, Mora MP, Raynaud C, *et al.* Control by osmotic pressure of voltage-induced permeabilization and gene transfer in mammalian cells. *Biophys J* 1998; 74: 3015–3022.
21. Imai E, Isaka Y. Gene electrotransfer: Potential for gene therapy of renal diseases. *Kidney Int* 2002; 61(Suppl 1): 37–41.
22. Kinosita K, Tsong TK. Formation and resealing of pores of controlled sizes in human erythrocyte membranes. *Nature* 1977; 268: 438–441.
23. Li LH, Ross P, Hui SW. Improving electrotransfection efficacy by postpulse centrifugation. *Gene Ther* 1999; 6: 364–372.
24. Li LH, McCarthy P, Hui SW. High-efficiency electrotransfection of human primary hematopoietic stem cells. *FASEB J* 2001; 15: 586–588.
25. Chang DG, Reese T. Changes of membrane structure induced by electroporation as revealed by rapid-freezing electron microscopy. *Biophys J* 1990; 58: 1–12.
26. Mir LM, Bureau MF, Gehl J, *et al.* High-efficiency gene transfer into skeletal muscle mediated by electric pulses. *Proc Natl Acad Sci U S A* 1999; 96: 4262–4267.

Kidney International, Vol. 63 (2003), pp. 501–513

Gene transfer of truncated IκBα prevents tubulointerstitial injury

Osamu Takase, Junichi Hirahashi, Atsushi Takayanagi, Akihiro Chikaraishi, Takeshi Marumo, Yuri Ozawa, Matsuhiko Hayashi, Nobuyoshi Shimizu, and Takao Saruta

Department of Internal Medicine and Department of Molecular Biology, Keio University Medical School, Tokyo, Japan

Gene transfer of truncated IκBα prevents tubulointerstitial injury.

Background. Severe proteinuria not only indicates the presence of progressive glomerular disease, but also causes tubular epithelial cells to produce inflammatory mediators leading to tubulointerstitial (TI) injury. We investigated the role of nuclear factor-κB (NF-κB) in tubular epithelial cells in the development of proteinuria-induced TI injury.

Methods. To specifically inhibit NF-κB activation, a recombinant adenovirus vector expressing a truncated form of IκBα (AdexIκBΔN) was injected into renal arteries of protein-overloaded rats, a model of TI injury characterized by infiltration of mononuclear cells and fibrosis.

Results. Activation of NF-κB in the renal cortex, observed in protein-overloaded rats treated with a control vector, recombinant lacZ adenovirus, was prevented in AdexIκBΔN-injected rats. Microscopic examination revealed AdexIκBΔN treatment to markedly attenuate proteinuria-induced TI injury. Increased immunostaining of vascular cell adhesion molecule-1, transforming growth factor-β, and fibronectin in TI lesions also was suppressed by AdexIκBΔN injection.

Conclusions. These findings provide evidence of the critical role of NF-κB activation in TI injury and suggest the therapeutic potential of adenovirus-mediated IκBΔN gene transfer into the kidney as a means of interrupting the process of TI damage.

Chronic renal disease with massive proteinuria is accompanied by tubulointerstitial injury and progressive deterioration of renal function [1, 2]. It is also known that, in patients with chronic glomerulonephritis, the decline in renal function correlates better with interstitial than with glomerular lesions [3]. The pathophysiological mechanisms underlying the tubulointerstitial injury in persistent proteinuria, however, remain unclear.

In recent years, several studies have indicated that filtered protein is reabsorbed and accumulated in proximal tubular cells, where it has an intrinsic renal toxicity [4]. Excessive protein loading of the proximal tubules results in the induction of genes encoding chemokines and cytokines, the expressions of which are regulated by the transcription factor, nuclear factor-κB (NF-κB) [2]. For example, rats with proteinuria induced by protein overload have been shown to exhibit an increase in renal monocyte chemoattractant protein 1 (MCP-1) expression in proximal tubules [5]. In vitro studies have shown that protein overload induces MCP-1 [6] and RANTES [7] in cultured proximal tubular cells in an NF-κB dependent manner. Indeed, activation of NF-κB in the kidney has been demonstrated in models of tubulointerstitial injury with proteinuria [8–10] and in patients with proteinuria [11]. Based on these findings, we consider the NF-κB pathway to be a potentially attractive target of therapeutic intervention for proteinuria-induced tubulointerstitial injury.

Although several agents including glucocorticoids, nonsteroidal anti-inflammatory drugs (NSAIDs), and antioxidants are known to inhibit NF-κB activation [12], the precise role of NF-κB activation needs to be addressed using a specific inhibitor of this pathway. In addition, since disruption of the subunits of NF-κB impairs the host immune response [13, 14], site-specific suppression of the NF-κB pathway may be required for therapeutic applications.

To specifically inhibit NF-κB activation, we used a recombinant adenovirus vector expressing the truncated form of IκBα (AdexIκBΔN), which lacks its N-terminal 54 amino acids including the phosphorylation sites essential for the activation of NF-κB [15]. With this adenovirus vector, we previously showed TNF-α–induced NF-κB activation to be strongly suppressed in rat mesangial cells [16] and human vascular smooth muscle cells [17] in vitro.

As a model of proteinuria, we used uninephrectomized rats with protein overload exhibiting tubulointerstitial injury characterized by accumulation of matrix proteins and infiltration of mononuclear inflammatory cells consisting mainly of monocytes and T-lymphocytes [5, 18]. Expression of vascular cell adhesion molecule-1 (VCAM-1), an NF-κB dependent molecule associated with localization and ac-

Key words: tubulointerstitial injury, nuclear factor-κB, adenovirus, proteinuria, progressive renal disease, inflammation.

Received for publication January 18, 2002
and in revised form August 7, 2002
Accepted for publication September 10, 2002

tivation of leukocytes in various inflammatory processes [19], was investigated in rats with protein overload. Adenovirus was injected via the renal artery since this route of adenoviral delivery has been shown to result in gene transfer exclusively into proximal tubular cells [20]. In this study, we determined the role of renal cortical NF-κB activation in proteinuria-induced injury.

METHODS

Recombinant adenovirus vector

A recombinant adenovirus vector was constructed that expressed the non-degraded form of the NF-κB inhibitor IκBα (Adex1CAKT IκBΔN; abbreviated AdexIκBΔN) as previously described [21]. This non-degraded IκBα (IκBΔN) lacked the 54 amino acids of the NH_2-terminus of wild-type human IκBα (MAD3). A modification of the cosmid-terminal protein complex method established by Dr. I. Saito (Tokyo University, Tokyo, Japan) [22] was used to construct this adenovirus vector. Purified virus stocks were prepared by cesium chloride (CsCl) step gradient centrifugation, as previously described [23]. A control vector, recombinant lacZ adenovirus (AdexlacZ) containing the CAG promotor, lacZ gene, which encodes *Escherichia coli* β-galactosidase, and polyA signal sequences, was kindly supplied by Dr. I. Saito [24].

Animals and experimental design

Female Wistar rats (six weeks old) were purchased from Charles River Japan (Tokyo, Japan) and housed individually in cages. They were fed CA-1 rat chow (27% protein; Clea Japan, Inc., Tokyo, Japan) and given free access to water. One week after a right uninephrectomy, the rats were laparotomized under general anesthesia, achieved with intraperitoneal injections of pentobarbital (10 mg/kg). After clipping the aorta both proximally and distally to the renal artery, AdexlacZ (1.0×10^8 PFU/mL) or AdexIκBΔ (5.0×10^7 PFU/mL) dissolved in 1 mL saline was injected into the renal artery and the clip was released three minutes after the injection. Control rats received injection of 1 mL saline without the virus.

In experiments determining the duration and localization of β-galactosidase expression, animals were killed by complete exsanguination under general anesthesia at day 7, 14, 21, or 28 after the injection of AdexlacZ. At the time of sacrifice, the remaining kidney was perfused with saline, decapsulated, and processed for X-gal staining.

To detect gene transfer of AdexIκBΔN into the renal cortex, rats were sacrificed at day 1, 4, or 7 after AdexIκBΔN infection. The renal cortex was excised from the perfused kidney, homogenized, quickly frozen in liquid nitrogen, and stored at −80°C for reverse transcription-polymerase chain reaction (RT-PCR) analysis. Rats injected with saline instead of virus were used as the control in this set of experiments.

In experiments investigating the effects of AdexIκBΔN administration on tubulointerstitial injury, uninephrectomized rats received daily intraperitoneal 2 g injections of bovine serum albumin (BSA; Sigma Chemical Company, St. Louis, MO, USA) starting one week after adenoviral infection. Control rats not injected with adenovirus were divided into two groups, a group injected with 2 g BSA and a group injected with an equivalent volume of saline. Rats were sacrificed at one, two, or three weeks after starting the BSA injections. After perfusion and decapsulation, the remaining kidney was bivalved. One section was cut into small pieces of cortex, snap frozen in liquid nitrogen, and stored at −80°C for determination of NF-κB activity. The other section was processed for histological and immunohistochemical analyses.

For determination of 24-hour urinary protein excretion and 24-hour creatinine clearance, fasting animals were placed in individual metabolic cages to collect urine. Blood was collected at the time of sacrifice for determinations of serum albumin, creatinine, and total cholesterol. Blood pressure was measured by tail-cuff plethysmography.

All procedures used in the animal experiments complied with the standards described in the *Guidelines for the Care and Use of Laboratory Animals* in Keio University School of Medicine.

X-gal staining

Coronal slices of each kidney were placed in O.C.T. embedding compound (Tissue-Tek; Sakura Finetek, Torrance, CA, USA), snap-frozen in liquid nitrogen, and stored at −80°C. Frozen sections, 8 μm in thickness, were cut with a cryostat and placed on poly-L-lysine-coated slides. The slices were fixed in Buffer A (0.2% glutaraldehyde, 0.1 mol/L potassium phosphate buffer, pH 7.4, 5 mmol/L EGTA, 2 mmol/L $MgCl_2$) at room temperature for five minutes. After three rinses with Buffer B (0.1 mol/L potassium phosphate buffer, pH 7.4, 0.02% Nonidet P40, 0.01% sodium-deoxycholate, 5 mmol/L EGTA, 2 mmol/L $MgCl_2$), the tissues were stained with X-gal solution [10 mmol/L $K_3Fe(CN)_6$, 10 mmol/L $K_4Fe(CN)_6$, 0.5 mg/mL 5-bromo-4-chloro-3-indolyl β-D-galactopyranoside; Sigma Chemical Company] in Buffer B (pH 7.4) at 37°C for 10 hours.

RT-PCR analysis

Total RNA was extracted from renal cortices with an RNA extraction kit, ISOGEN (Nippon Gene Co., Tokyo, Japan), according to the manufacturer's instructions. RNA isolated from each group was treated with RNase-free DNase, and cDNA was synthesized with a commercial kit (Ready To Go™ T-Primed First-Standard Kit; Amersham Pharmacia Biotech Inc., Tokyo, Japan). The cDNA product was amplified by PCR with the use of primers for AdexIκBΔN (sense primer, 5'-CTCCAGCA

GACTCCACTCCACT-3', and antisense primer, 5'-ACA CCAGCCACCACCTTCTGAT-3'), yielding a 712 bp fragment. The PCR was initiated by a five minute incubation at 95°C, followed by 35 cycles of one minute at 95°C, one minute 30 seconds at 60°C, and one minute 30 seconds at 72°C. The resulting reaction products were analyzed by gel electrophoresis (1% agarose) using a 100 bp ladder as a size marker.

Histological analysis

Coronal sections of renal tissue were immersion-fixed in 10% neutral-buffered formalin and embedded in paraffin. Sections were stained with periodic acid Schiff (PAS) to determine cellular infiltration and Masson's trichrome for fibrotic changes, and then viewed with a microscope. The severity of tubulointerstitial scarring and glomerulosclerosis was graded semiquantitatively (1 through 4) in a blinded manner, and the mean score was calculated according to a previously described scoring method [25, 26]. Tubulointerstitial scarring was scored as follows: 1 = normal tubules and interstitium; 2 = mild tubular atrophy and interstitial fibrosis; 3 = moderate tubular atrophy and dilation with marked interstitial fibrosis; 4 = end-stage kidney with extensive interstitial fibrosis and few remaining atrophic tubules. A score was given to each microscopic field viewed at a magnification of ×200. The glomerulosclerosis scoring system was as follows: 1 = normal glomeruli; 2 = presence of mild segmental glomerulosclerosis affecting <25% of the glomerular tuft; 3 = moderate segmental sclerosis affecting 25 to 50% of the glomerular tuft; 4 = diffuse severe glomerulosclerosis affecting >50% of the tuft, including glomeruli with total tuft obliteration, fibrosis, and obsolescence. The scores for tubulointerstitial scarring and glomerulosclerosis in each rat were obtained by the examination of 25 to 50 cortical fields and glomeruli, respectively, per kidney. The mean number of interstitial mononuclear cells was calculated in a blinded manner by averaging the total number of mononuclear cells in the interstitium in 30 randomly selected high-power (×200) cortical fields as previously described [27].

Immunohistochemistry of VCAM-1, transforming growth factor-β, and fibronectin

Expression of VCAM-1, transforming growth factor-β (TGF-β), and fibronectin was detected by immunostaining according to a previously described method [28], with minor modifications. Coronal sections of renal tissue were immersion-fixed in 4% buffered-paraformaldehyde for 12 hours and washed with 10%, 15%, and 20% sucrose in phosphate-buffered saline (PBS) for four hours each time and then embedded in O.C.T. These sections were snap-frozen in liquid nitrogen, and stored at −80°C. Frozen sections, 8 μm in thickness, were cut with a cryostat and air dried. After being washed in PBS (pH 7.4), the sections were blocked sequentially with 0.3% H_2O_2 in methanol and 2% normal goat serum. The sections were incubated at room temperature for two hours with rabbit anti-VCAM-1 (dilution 1:400; Santa Cruz Biotechnology, Inc., Santa Cruz, CA, USA), rabbit anti-rat TGF-β (dilution 1:500; R&D Systems, Minneapolis, MN, USA), or rabbit anti-rat fibronectin (dilution 1:500; Chemicon International, Temecula, CA, USA) polyclonal antibodies as the primary antibodies. After three rinses with PBS, goat anti-rabbit biotinylated secondary antibody at 1:1000 dilutions was applied to the sections for 60 minutes. The sections were then reacted with streptavidin-biotinylated peroxidase complex for 30 minutes, and stained with tetramethylbenzidine for horseradish peroxidase histochemistry. After washing and cover slipping on glycerol, the sections were examined under a microscope within 24 hours. For evaluation of the immunostaining of TGF-β and fibronectin, each tubulointerstitial grid field was graded semiquantitatively (0 through 4) in a blinded manner and the mean score was calculated according to a previously described scoring method [29–31].

Extraction of nuclear proteins from renal cortex homogenates

Nuclear protein extracts from cortical tissue were prepared according to a previously described method [32], with minor modifications [8]. Two hundred mg of cortical tissue were homogenized with a glass Teflon homogenizer in 400 μL of ice-cold buffer A [10 mmol/L HEPES, pH 7.9, 10 mmol/L mol/L KCl, 2 mmol/L $MgCl_2$, and 0.1 mmol/L ethylenediaminetetraacetic acid (EDTA)], a protease inhibitor cocktail tablet (Roche Molecular Biochemicals, Mannheim, Germany)] followed by addition of 65 μL of 2% Nonidet-P40. The mixture was vortexed, and then centrifuged at 13,000 × *g* for five minutes. The supernatant was removed, and the pellet was resuspended in 60 μL of Buffer B [50 mmol/L HEPES, 10% (vol/vol) glycerol, 300 mmol/L NaCl, 50 mmol/L KCl, a protease inhibitor cocktail tablet]. The mixture was centrifuged at 13,000 × *g* for 10 minutes. The supernatant included nuclear protein, and was diluted to a standard concentration of 3 μg/μL. The protein concentrations were determined by the Bradford method (Bio-Rad Laboratories. Hercules, CA, USA) [33].

Electrophoretic mobility shift assay and densitometry

Double stranded NF-κB consensus oligonucleotides (5'-AGTTGAGGGGACTTTCCCAGGC-3'; Promega, Madison, WI, USA) were end labeled with [^{32}P]-γ-ATP (Amersham Life Science Inc. Sydney, Australia). Unincorporated label was removed with a QIAquick spin column (Qiagen K.K., Valencia, CA, USA). The binding reaction was performed for 30 minutes at room temperature and the binding mixture contained 5 μg of nuclear protein extract, 2 μL of gel shift binding 5× buffer [20%

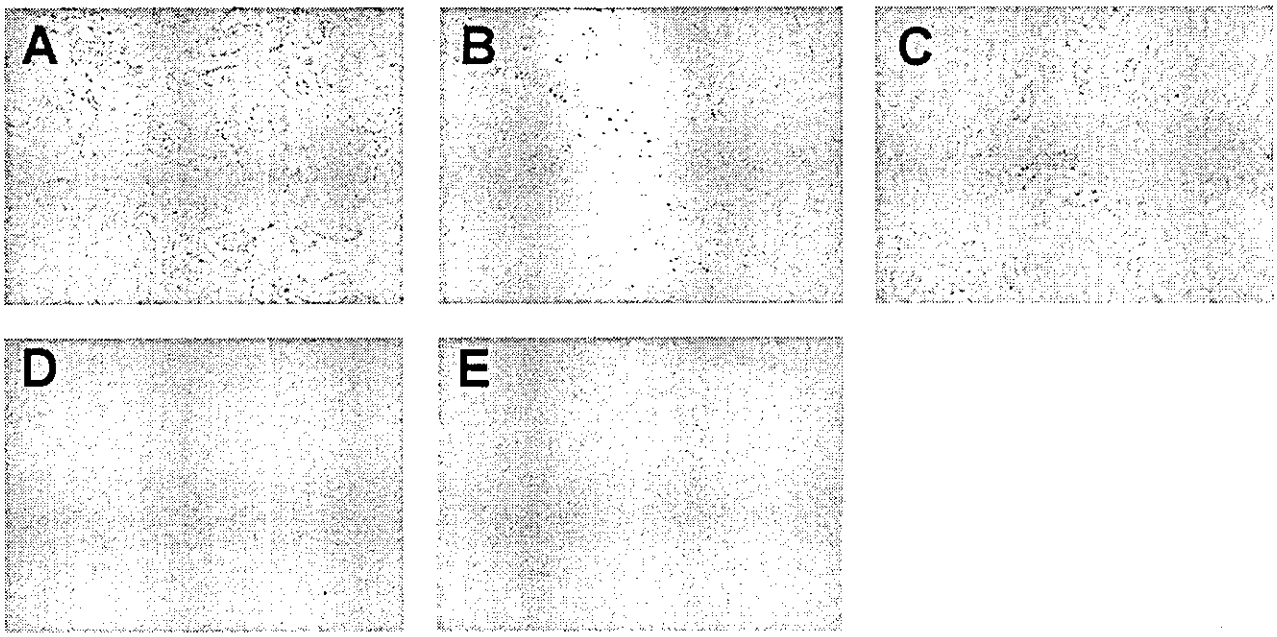

Fig. 1. In vivo gene transfer of β-galactosidase into proximal tubular cells. AdexlacZ was injected into the renal artery and the expression of β-galactosidase was detected as a blue area in tubular epithelial cells 7 (*A*), 14 (*B*), and 21 (*C*) days after adenoviral injection (original magnification ×100). There was no X-gal staining in the liver of a rat 7 days after injection of AdexlacZ into the renal artery (*D*, original magnification ×100) or in the renal cortex of a rat 7 days after injection of saline into the renal artery (*E*, original magnification ×100).

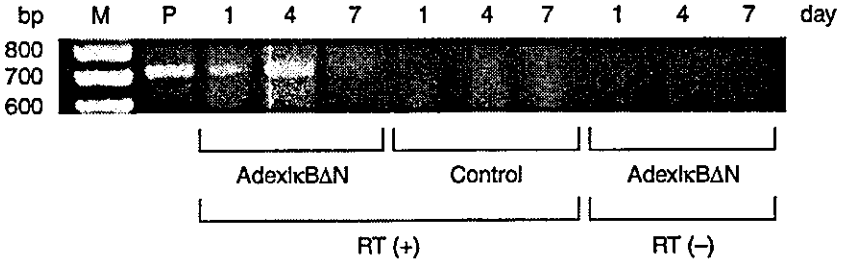

Fig. 2. Reverse transcription-polymerase chain reaction (RT-PCR) of renal cortical mRNA for IκBΔN transcripts. RT-PCR was performed with total RNA extracted from the renal cortices of rats 1, 4, and 7 days after injection of AdexIκBΔN or saline (control) in the presence and absence of reverse transcriptase (RT). As a positive control, the product from AdexIκBΔN itself was included (P).

glycerol, 5 mmol/L $MgCl_2$, 2.5 mmol/L EDTA, 2.5 mmol/L dithiothreitol (DTT), 250 mmol/L NaCl, 50 mmol/L Tris-HCl (pH 7.5), 0.25 mg/mL poly[dI-dC]-poly[dI-dC] and 1 μL of ^{32}P-labeled (50,000 cpm counting) oligonucleotides in a total volume of 10 μL. In the competition assays, a 100-fold excess of unlabeled NF-κB consensus or mutant NF-κB oligonucleotides (5′-AGTTGAGGC AACGGTCCCAGGC-3′) was added to labeled NF-κB consensus oligonucleotides. After the addition of 1 μL of gel-loading buffer (250 mmol/L Tris-HCl, pH 7.5, 0.2% bromophenol blue, 40% glycerol), the DNA-protein complexes were resolved by electrophoresis on a 7% polyacrylamide gel in TBE buffer as previously described [34]. The gel was run at 150 V for 90 minutes and then dried at 80°C with a gel drier. Autoradiographs were prepared by exposing the dried gel to X-ray film with intensifying screens for three to six hours at room temperature. The density of specific NF-κB complex was determined with a laser scanning densitometer and image analysis software (BAStation; Fuji Photo Film Co., Ltd., Tokyo, Japan) as previously described [35].

Western blot analysis of VCAM-1

Vascular cell adhesion molecule-1 protein levels in cortical tissue were determined according to a previously described method [16], with minor modifications. In brief, cortical tissue was homogenized in Tris buffer with proteinase inhibitors (Roche Molecular Biochemicals). After determination of the protein concentration with the Bio-Rad protein assay kit, protein samples (40 μg) were mixed with reducing buffer, heated at 100°C for five minutes and then subjected to 7.5% SDS-PAGE. The separated proteins were electrophoretically transferred to nitrocellulose membranes. The blots were blocked in 5%

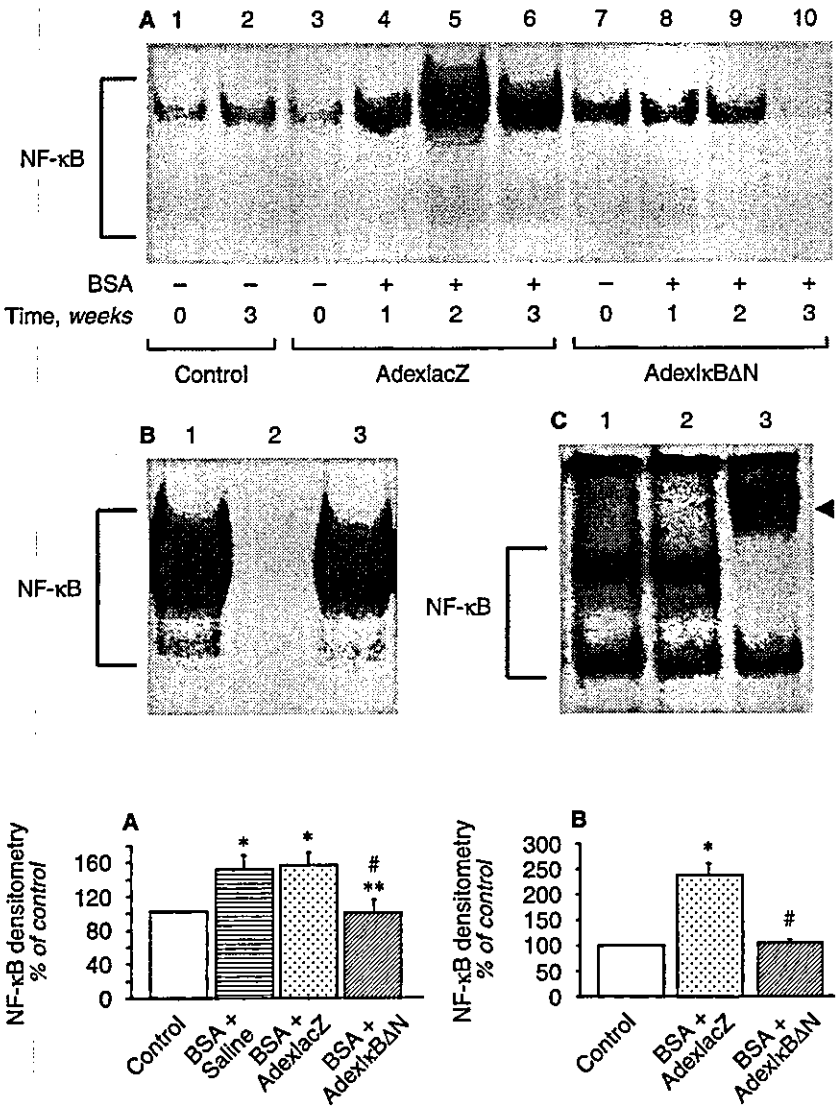

Fig. 3. Time course of nuclear factor-κB (NF-κB) activity in protein-overloaded rats. A representative autoradiogram of an electrophoretic mobility shift assay for NF-κB in nuclear extracts from the renal cortex at 0 to 3 weeks after the start of daily bovine serum albumin (BSA) injections is shown (*A*). Lanes 1 and 2, rats at 0 and 3 weeks of daily intraperitoneal saline injection (control); lanes 3 to 6, AdexlacZ-treated rats at 0 to 3 weeks of protein overload; lanes 7 to 10, AdexIκBΔN-treated rats at 0 to 3 weeks of protein overload. Competition assay was performed to determine the binding specificity of the NF-κB oligonucleotides (*B*). The binding reactions were performed with nuclear proteins from AdexlacZ-treated rats at 3 weeks of protein overload (lane 1), in the presence of a 100-fold excess of unlabeled consensus (lane 2) or mutant (lane 3) oligonucleotide competitors. Nuclear extracts obtained from AdexlacZ-treated rats at 3 weeks of protein overload were incubated with or without (lane 1) anti-p50 (lane 2) or anti-p65 (lane 3) antibody and analyzed for NF-κB binding activity. Brackets indicate the positions of specific NF-κB complex. An arrowhead indicates the position of supershifted complex.

Fig. 4. Densitometric analysis of the autoradiographic results at one (*A*) and three (*B*) weeks of protein overload. Values obtained from electrophoretic mobility shift assays for NF-κB in nuclear extracts from the renal cortex at one and three weeks after the start of daily bovine serum albumin (BSA) injections were normalized and expressed as percentages of the control. Control rats were injected with saline daily. Rats loaded with BSA had been injected with saline, AdexlacZ or AdexIκBΔN one week before the start of protein overload. Data are means ± SEM from 4 rats. $*P < 0.05$ vs. control values. $\#P < 0.05$ vs. values of saline-treated rats with BSA loading. $**P < 0.05$ vs. values of AdexlacZ-treated rats.

nonfat milk and incubated for four hours at 22°C with the primary polyclonal antibody against VCAM-1 (dilution 1:100; Santa Cruz Biotechnology), and then for one hour with a secondary antibody conjugated to horseradish peroxidase (dilution 1:500; Amersham Life Science). Immunoreactive bands were visualized by enhanced chemiluminescence (ECL; Amersham Life Science). Densitometric analysis was performed with the NIH image program (Bethesda, MD, USA).

Statistics

All data are expressed as means ± SEM. Multiple parametric comparisons were evaluated by analysis of variance (ANOVA), followed by Fisher's protected least significant difference test. The scores for tubulointerstitial scarring, glomerulosclerosis, and immunostaining were compared by Kruskal-Wallis test, followed by the Mann-Whitney U test. Values of $P < 0.05$ were considered statistically significant.

RESULTS

In vivo gene transfer of β-galactosidase into tubular cells

As previously described [20], injection of AdexlacZ into renal artery resulted in the expression of β-galactosidase in tubular epithelial cells at day 7, as shown in Figure 1A. The expression of β-galactosidase gradually decreased at days 14 and 21 (Fig. 1 B, C) and only few β-galactosidase-positive cells were found at day 28 (data not shown). The expression of β-galactosidase was not observed in either glomerular or interstitial areas at any time. No β-galactosidase-transduced cells could be detected in

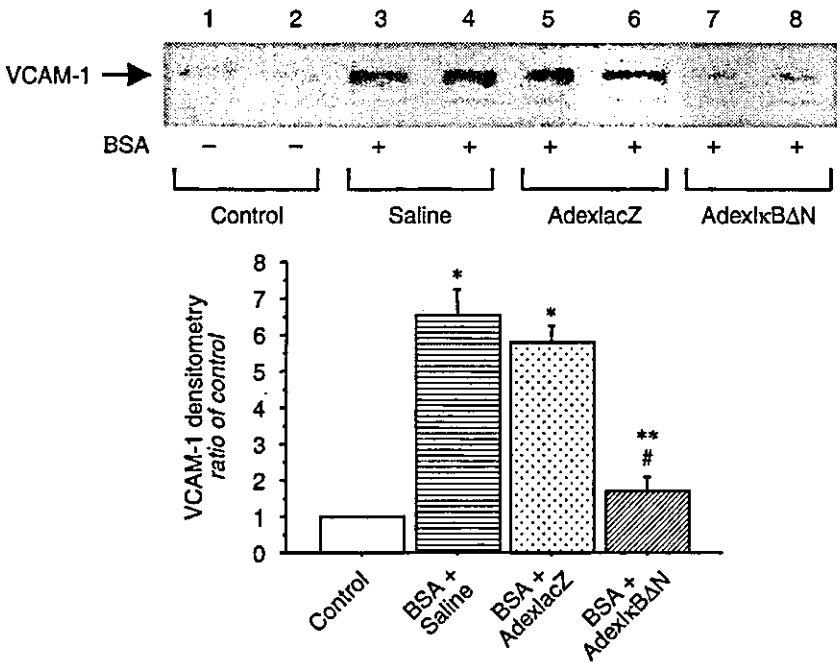

Fig. 5. Cortical expression of VCAM-1 after one week of protein overload. Protein levels of VCAM-1 in the cortical tissue were determined by Western blotting and are shown in the upper panel. Lanes 1 and 2, rats after one week of daily intraperitoneal saline injections; lanes 3 and 4, saline-injected rats after one week of protein overload; lanes 5 and 6, AdexlacZ-injected rats after one week of protein overload; lanes 7 and 8, AdexIκBΔN-injected rats after one week of protein overload. As shown in the lower panel, values obtained by densitometric analysis of Western blots for VCAM-1 were normalized and expressed as percentages of the control. Data are means ± SEM from 3 rats. $*P < 0.05$ vs. control values; $\#P < 0.05$ vs. values of saline-injected rats with protein overload; $**P < 0.05$ vs. values of AdexlacZ-injected rats.

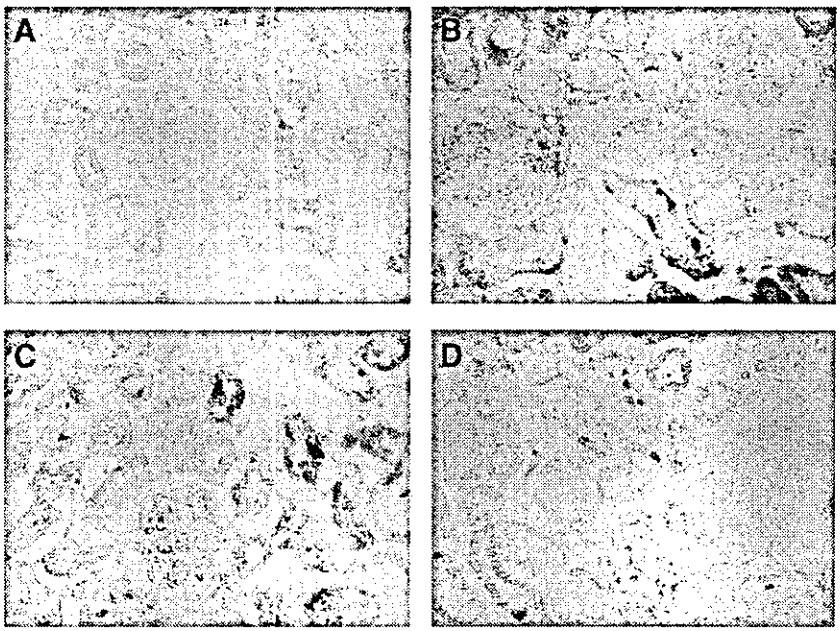

Fig. 6. Representative photomicrographs of VCAM-1 immunostaining in kidney sections after one week of protein overload. (*A*) Rats without protein overload. (*B*) Saline-injected rats with protein overload. (*C*) AdexlacZ-injected rats with protein overload. (*D*) AdexIκBΔN-injected rats with protein overload (original magnification ×200).

other organs including liver (Fig. 1D) and heart (data not shown). There was no X-gal staining in the cortex of rats injected with saline instead of AdexlacZ (Fig. 1E).

Expression of IκBΔN in the renal cortex

Transcription of AdexIκBΔN was detected by RT-PCR using specific primers. RNA extracted from the cortices at one, four, and seven days after AdexIκBΔN injection was reverse transcribed and amplified using specific primers. As shown in Figure 2, the 712 bp fragment was amplified from AdexIκBΔN-injected group samples, but not from control samples. Although the intensity of the band tended to be decreased on day 7, a faint band of AdexIκBΔN still could be detected. No

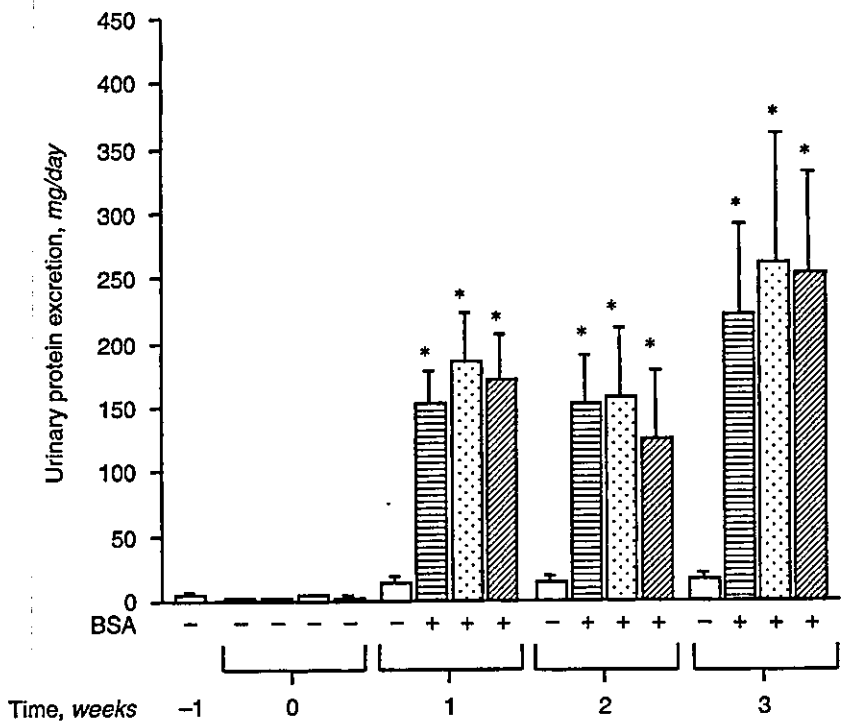

Fig. 7. Time course of urinary protein excretion of rats with (+) or without (−; □) bovine serum albumin (BSA) loading. Rats loaded with BSA had been injected with saline (▨), AdexlacZ (▩), or AdexIκBΔN(▤) one week before the start of protein overload. *$P <$ 0.05, vs. control values.

Table 1. Biochemical profile of rats with or without (control) protein overload for 3 weeks

	Control	Saline	AdexlacZ	AdexIκBΔN
Body weight *g*	244 ± 26.7	208 ± 9.6	227 ± 15.0	234 ± 19.1
Kidney weight *g*	1.75 ± 0.19	2.42 ± 0.27[a]	2.89 ± 0.19[a]	2.04 ± 0.18[c]
Kidney/body weight %	0.72 ± 0.14	1.15 ± 0.79[a]	1.27 ± 0.28[a]	0.87 ± 0.46[b,c]
Blood pressure *mm Hg*	119 ± 6.8	127 ± 5.3	144 ± 9.9	140 ± 15.9
Serum albumin *g/dL*	3.80 ± 0.13	5.18 ± 0.39[a]	4.93 ± 0.39[a]	5.00 ± 0.40[a]
Total cholesterol *mg/dL*	66.2 ± 5.41	64.8 ± 5.36	76.0 ± 5.51	56.0 ± 7.62
Serum creatinine *mg/dL*	0.35 ± 0.02	0.36 ± 0.03	0.33 ± 0.03	0.36 ± 0.04
24-Hour C_{Cr} *mL/min*	1.26 ± 0.17	1.23 ± 0.10	1.45 ± 0.13	1.13 ± 0.26

Rats with protein overload had been injected with saline, AdexlacZ as a control vector or AdexIκBΔN one week before the start of protein overload. Data represent mean values ± SEM from 5 rats of each group. 24-Hour C_{Cr} is 24-hour creatinine clearance.

[a] $P < 0.05$ vs. control values

[b] $P < 0.05$ vs. values of saline-treated group

[c] $P < 0.05$ vs. values of AdexlacZ-treated group

bands of this size were obtained from the AdexIκBΔN-injected group samples without reverse transcriptase.

Time course of cortical NF-κB activation in proteinuric rats

Nuclear factor-κB DNA-binding activities were assessed in whole cortical nuclear extracts from rats with and without protein overload by EMSA (Fig. 3). In rats without a protein overload, the incubation of cortical nuclear extracts with labeled consensus NF-κB oligonucleotides produced weak bands (Fig. 3A, lanes 1 and 2). The activation of NF-κB was induced at one week, peaked at two weeks, and persisted for at least three weeks after initiating protein overload in AdexlacZ-treated rats (Fig. 3A, lanes 3 to 6). By contrast, in AdexIκBΔN-injected rats, NF-κB activation was markedly reduced (Fig. 3A, lanes 7 to 10). As shown in Figure 3B, the NF-κB/DNA bands were abolished by the unlabeled consensus oligonucleotides, but not by the mutant oligonucleotides. Treatment of nuclear extracts with a specific anti-p65 antibody resulted in a supershift of the NF-κB/DNA bands, demonstrating the presence of p65 in the bands (Fig. 3C). By contrast, antibody to p50 did not produce any change in the NF-κB/DNA bands. Densitometric analysis revealed the treatment of proteinuric rats with AdexIκBΔN to prevent the cortical activation of NF-κB at one and three weeks (Fig. 4). The cortical activation of NF-κB in the proteinuric rats that had not

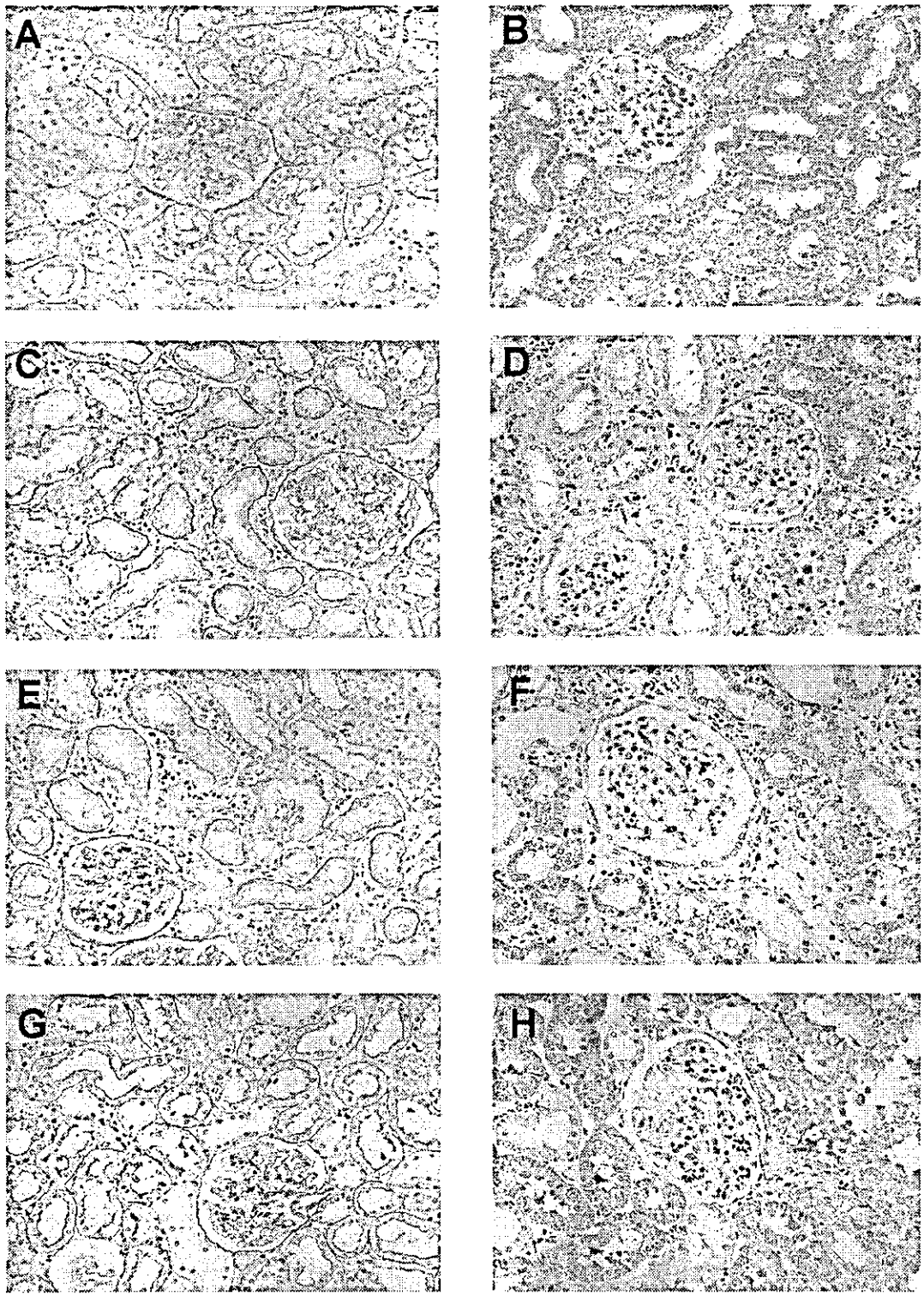

Fig. 8. Representative photomicrographs of periodic acid-Schiff (*A, C, E,* and *G*) and Masson's trichrome (*B, D, F,* and *H*) staining of kidney sections at 3 weeks after the start of protein overload. (A and B) Rats without protein overload. (C and D) Saline-injected rats with protein overload. (E and F) AdexlacZ-injected rats with protein overload. (G and H) AdexIκBΔN-injected rats with protein overload (original magnification ×200).

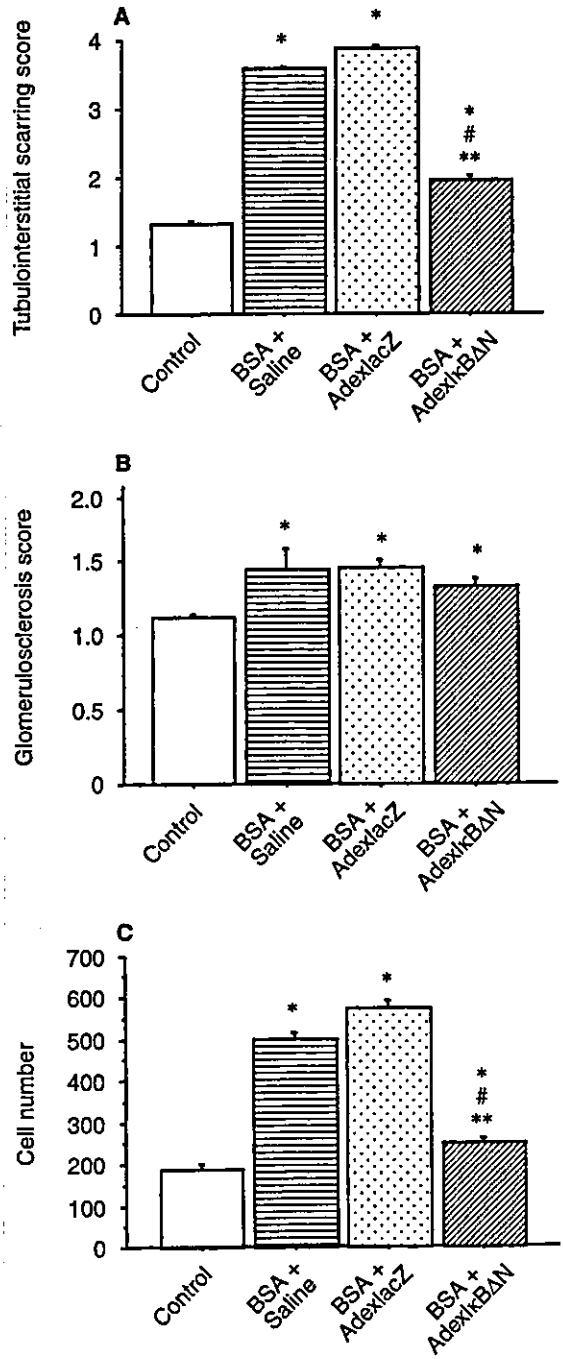

Fig. 9. Tubulointerstitial scarring and glomerulosclerosis scores and number of interstitial mononuclear cells in rats with or without protein overload for 3 weeks. Rats with protein overload had been injected with saline, AdexlacZ, or AdexIκBΔN one week before the start of protein overload. Data are means ± SEM from 5 rats. $*P < 0.05$ vs. control values; $\#P < 0.05$ vs. values of saline-injected rats with protein overload; $**P < 0.05$ vs. values of AdexlacZ-injected rats.

been injected with adenovirus was similar in extent to the activation in the AdexlacZ group at one week.

Expression of VCAM-1

To investigate whether AdexIκBΔN attenuated induction of an NF-κB dependent molecule, we examined the cortical expression of VCAM-1 in the early phase of the renal injury. Western blot analysis revealed that protein overload induced marked increases in VCAM-1 protein in the renal cortical tissue of saline- and AdexlacZ-injected rats (Fig. 5). As shown in Figure 6, the up-regulation of VCAM-1 was mainly observed in proximal tubular cells, with marked induction in the basolateral portion of the epithelium. Occasional expression of VCAM-1 also was observed in glomerular and interstitial areas. The levels of VCAM-1 protein were significantly lower in rats injected with AdexIκBΔN (Figs. 5 and 6).

Biochemical profile

As shown in Figure 7, protein-overloaded rats developed significant proteinuria. The levels of urinary protein excretion did not differ significantly among groups injected with saline, AdexlacZ, and AdexIκBΔN during the course of BSA overload. Kidney weight and the ratio of kidney/body weight were significantly greater in protein-overloaded rats that had been injected with saline or AdexlacZ than in the control group (Table 1). The increase in the ratio of kidney/body weight was significantly attenuated in the AdexIκBΔN-treated group compared to the saline- and AdexlacZ-treated groups. Serum albumin levels of rats with protein overload were significantly higher than those of controls. Blood pressure, total cholesterol, serum creatinine, and 24-hour creatinine clearance did not differ significantly among the groups at sacrifice.

Light microscopy studies

In accordance with previous reports [5, 18], light microscopic analysis revealed protein overload to induce marked tubulointerstitial injury in the renal cortices of saline- and AdexlacZ-injected rats at three weeks (Fig. 8). The tubular changes consisted of tubular cell brush border loss, cellular atrophy, and basement membrane thickening. The interstitial space was expanded due to an increase in mononuclear inflammatory cell infiltration, interstitial edema, and fibrosis. In contrast, kidneys injected with AdexIκBΔN showed minor tubulointerstitial injury as compared to the saline- and AdexlacZ-injected groups. Sections were scored according to the severity of tubulointerstitial scarring and glomerulosclerosis at three weeks after protein overload (Fig. 9). While protein overload induced a marked increase in the tubulointerstitial scarring score in the saline- and AdexlacZ-treated groups, the increase in the score was significantly attenuated in rats infected with AdexIκBΔN. There was

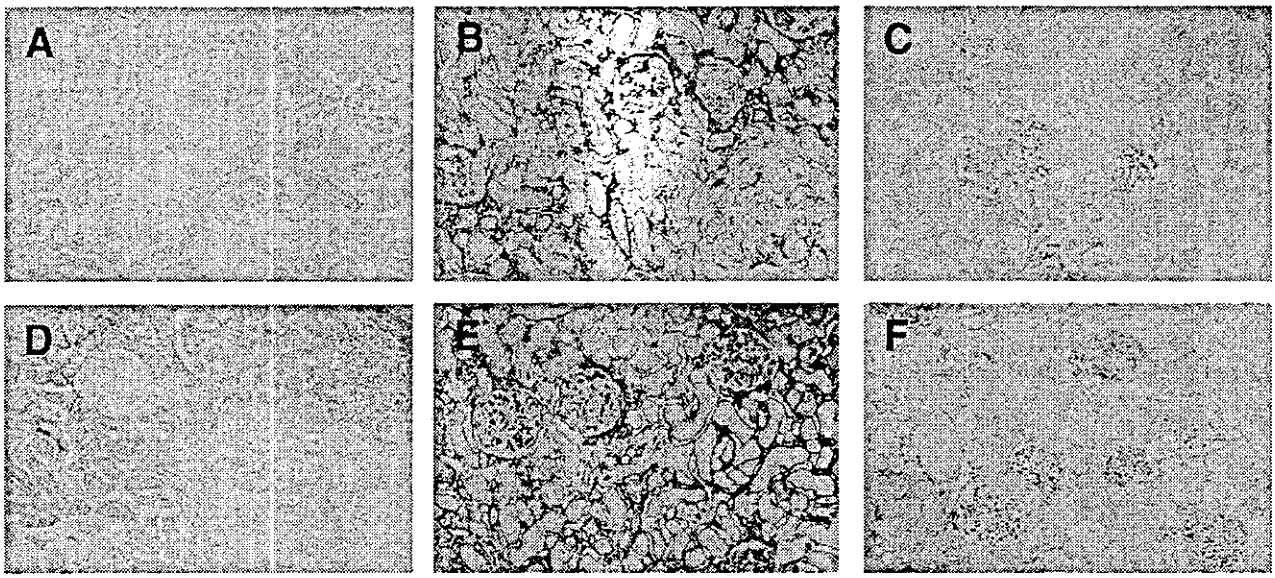

Fig. 10. Representative photomicrographs of immunostaining for TGF-β (*A, B, and C*) and fibronectin (*D, E, and F*) in kidney sections at three weeks after protein overload. (A and D) Rats without protein overload. (B and E) AdexlacZ-treated rats with protein overload. (C and F) AdexIκBΔN-treated rats with protein overload (original magnification ×100).

a slight increase in the glomerulosclerosis score in proteinuric rats, but no significant differences were observed among the groups. The number of interstitial mononuclear cells was increased in the saline- and AdexlacZ-treated groups, while the increase was markedly attenuated in rats injected with AdexIκBΔN (Fig. 9).

Expression of TGF-β and fibronectin

Since increased levels of interstitial TGF-β and fibronectin were reportedly associated with interstitial fibrosis in uninephrectomized rats with protein overload [5], we next investigated the expressions of these proteins. Strong focal and segmental staining for TGF-β and fibronectin was observed in the interstitial space in AdexlacZ-infected rats, whereas staining was much less intense in AdexIκBΔN-infected rats (Fig. 10). No significant staining was observed without primary antibodies (data not shown). Semiquantitative scoring revealed that tubulointerstitial immunostaining scores for TGF-β and fibronectin were significantly lower in rats treated with AdexIκBΔN than in AdexlacZ-treated rats (Fig. 11). Weak staining for TGF-β and fibronectin in the glomeruli of proteinuric rats also was identified, but there were no differences between the AdexlacZ and AdexIκBΔN-infected groups.

DISCUSSION

This study demonstrates that NF-κB activation in the renal cortex plays a critical role in tubulointerstitial injury induced by proteinuria. The present results also suggest the possibility of AdexIκBΔN being utilized as a therapeutic tool.

To investigate the process of tubulointerstitial injury associated with proteinuria, we selected a non-immunogenic rat model of tubulointerstitial injury induced by protein overload. Since the levels of protein excretion did not differ between the AdexIκBΔN and AdexlacZ groups, tubular epithelial cells were considered to have been subjected to the same protein load in both groups. This finding indicates that our experimental conditions were appropriate for investigating the role of NF-κB activation in the formation of tubulointerstitial injury induced by protein overload.

Previous reports have demonstrated that the distribution of gene products transduced by adenovirus in the kidney depends on the conditions of viral administration and on the transfected species. When the adenoviral vector is infused via the rat ureter, tubular cells in the papilla and medulla are the predominant sites of transduction [20]. While Sukhatme's group successfully transduced a reporter gene in rat renal vasculature by infusing the adenovirus via the renal artery with venous clamping and cold incubation [36], interstitial cells in the cortex are mainly transfected when a similar method is applied to dogs [37]. Glomerular cells have been reported to be transfected also when porcine kidney is continuously perfused for two hours [38]. In agreement with the finding by Moullier et al [20], we observed that the injection of adenovirus into the rat renal artery with arterial clamping resulted in a selective gene transfer into proximal tubular cells. Although Moullier et al reported a

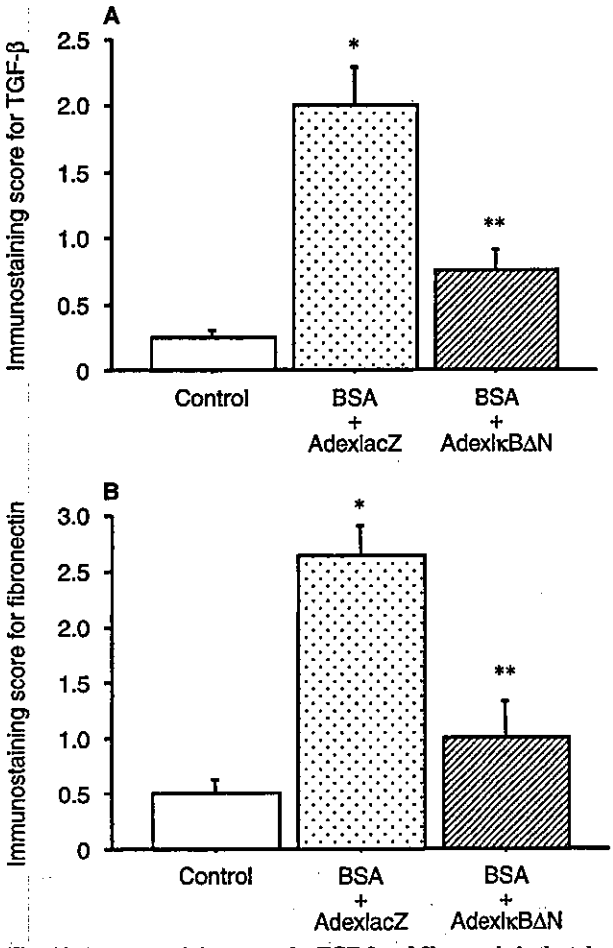

Fig. 11. Immunostaining scores for TGF-β and fibronectin in the tubulointerstitial space of rats with or without protein overload. Rats with protein overload had been injected with AdexlacZ or AdexIκBΔN one week before the start of protein overload. Data represent mean values ± SEM from 4 rats. $^{*}P < 0.05$ vs. control values; $^{**}P < 0.05$ vs. values of AdexlacZ-treated rats.

rather heterogeneous transduction of β-galactosidase in tubular cells, we observed a homogeneous distribution of β-galactosidase-positive cells in renal cortex. The reason for the discrepancy between these results is unclear. However, the status of the intrarenal hemodynamics seems to be particularly important in determining the distribution of adenoviral infection, since co-administration of vasodilators with adenovirus has been reported to induce a significant change in the distribution of transferred gene products in the kidney [36]. Thus, the altered renal circulation caused by the heminephrectomy that was performed prior to transfection in our study may have contributed to the homogeneous distribution of adenovirus in the renal cortex.

Treatment with AdexIκBΔN prevented the NF-κB activation observed in AdexlacZ-injected rats throughout the course of protein overload. Expression of IκBΔN transcripts in the renal cortices of the AdexIκBΔN-injected group was confirmed by RT-PCR analysis up until 7 days after the administration of the adenovirus. However, the IκBΔN mRNA levels seemed to be decreased on day 7. These results suggest that IκBΔN protein levels sufficient to prevent NF-κB activation may be maintained during the course of the renal injury despite the decrease in the mRNA levels in the early stage. In rats with protein overload, tubular cells have been shown to be the major source of NF-κB during the early stage of interstitial injury, beginning as early as 24 hours after the start of protein overload [10]. This report, together with the present results concerning the distribution of β-galactosidase in tubular cells, supports the idea that AdexIκBΔN treatment prevents NF-κB activation in tubular cells during the early stage of interstitial injury induced by protein overload. This notion is supported further by the present finding that the increase in tubular levels of VCAM-1, the expression of which is controlled by NF-κB in renal epithelial cells [39], was attenuated by AdexIκBΔN after one week of protein overload.

The present study demonstrates that the inhibition of the NF-κB pathway in the renal cortex by AdexIκBΔN attenuates tubulointerstitial injury, including interstitial infiltration of mononuclear cells, in proteinuric rats. Since VCAM-1 mediates localization and stimulation of inflammatory cells [40, 41] and its expression is related to the degree of tubulointerstitial injury in human glomerulonephritis [42], inhibition of VCAM-1 expression by AdexIκBΔN probably contributes to the attenuation of tubulointerstitial injury to some extent. In addition to VCAM-1, other NF-κB dependent molecules, such as MCP-1 and RANTES [6, 7], may play some role in the development of NF-κB dependent tubulointerstitial injury induced by protein overload, although the precise contributions of the various proinflammatory molecules remain to be elucidated.

The reduced ratio of kidney weight/body weight in rats treated with AdexIκBΔN, as compared to the saline and AdexlacZ groups, indicates that the inhibition of NF-κB activation attenuates renal hypertrophy in proteinuric rats. In line with this observation, the histological analysis revealed that interstitial fibrosis in proteinuric rats was reduced in rats treated with AdexIκBΔN. These effects of AdexIκBΔN in part may be due to a reduction in the interstitial expression of TGF-β, a profibrogenic cytokine, and fibronectin, an interstitial matrix protein, as demonstrated by immunostaining. Since interstitial inflammatory cells have been shown to produce TGF-β in rats with protein overload [5], the attenuated infiltration of mononuclear cells is likely to contribute to the reduction in TGF-β staining observed in the AdexIκBΔN group.

Largo et al reported the up-regulation of angiotensin-converting enzyme and angiotensinogen in proximal tu-

bules of rats made proteinuric with protein overload, and suggested local production of angiotensin II to play a role in the tubulointerstitial injury in this model [28]. Angiotensin II appears to participate in renal interstitial fibrosis by stimulating production of TGF-β and fibronectin in renal interstitial cells [43]. Since transcription of angiotensinogen gene is controlled by NF-κB [44], decreased local generation of angiotensin II also may contribute to the attenuated expression of TGF-β and fibrosis in the AdexIκBΔN group.

Possible involvement of NF-κB activation in tubulointerstitial injury in proteinuric rats was suggested in a recent report demonstrating that the administration of pyrrolidine dithiocarbamate (PDTC), an antioxidant, inhibits renal NF-κB activation and tubulointerstitial injury induced by adriamycin [8], an oxidant known to deplete cellular glutathione [45]. The specificity of PDTC as an inhibitor of NF-κB is questionable, however, since PDTC increases intracellular glutathione levels [46] and also acts as a metal chelator [47]. In this regard, the present study provides direct evidence that NF-κB activation is involved in tubulointerstitial injury associated with proteinuria.

In conclusion, our present study shows that the adenovirus-mediated gene transfer of mutant IκB prevented tubulointerstitial injury induced by protein overload. This result demonstrates the important role of NF-κB activation in tubulointerstitial injury and also suggests the possibility of using gene therapy targeting NF-κB for the treatment of tubulointerstitial injury associated with glomerulonephritis.

ACKNOWLEDGMENTS

This work was supported in part by a grant-in-aid from the Ministry of Education, Culture, Sports, Science and Technology of Japan, Health Science Research Grants from the Ministry of Health, Labor and Welfare, and a Grant for Fundamental Research Program for Advanced Medical Apparatus Undertaken in Cooperation with Medical and Engineering Researchers from the New Energy and Industrial Technology Development Organization (NEDO). Portions of this work were presented at the 33rd Annual Scientific Meeting of the American Society of Nephrology, Toronto, Canada.

Reprint requests to Matsuhiko Hayashi, M.D., Department of Internal Medicine, Keio University Medical School, 35 Shinanomachi, Shinjukuku, 160-8582 Tokyo, Japan.
E-mail: matuhiko@sc.itc.keio.ac.jp

REFERENCES

1. Remuzzi G, Bertani T: Is glomerulosclerosis a consequence of altered glomerular permeability to macromolecules? *Kidney Int* 38:384–394, 1990
2. Remuzzi G, Ruggenenti P, Benigni A: Understanding the nature of renal disease progression. *Kidney Int* 51:2–15, 1997
3. Becker GJ, Hewitson TD: The role of tubulointerstitial injury in chronic renal failure. *Curr Opin Nephrol Hypertens* 9:133–138, 2000
4. Remuzzi G: Abnormal protein traffic through the glomerular barrier induces proximal tubular cell dysfunction and causes renal injury. *Curr Opin Nephrol Hypertens* 4:339–342, 1995
5. Eddy AA, Giachelli CM: Renal expression of genes that promote interstitial inflammation and fibrosis in rats with protein-overload proteinuria. *Kidney Int* 47:1546–1557, 1995
6. Wang Y, Rangan GK, Tay YC, Harris DC: Induction of monocyte chemoattractant protein-1 by albumin is mediated by nuclear factor κB in proximal tubule cells. *J Am Soc Nephrol* 10:1204–1213, 1999
7. Zoja C, Donadelli R, Colleoni S, *et al*: Protein overload stimulates RANTES production by proximal tubular cells depending on NF-κB activation. *Kidney Int* 53:1608–1615, 1998
8. Rangan GK, Wang Y, Tay YC, Harris DC: Inhibition of nuclear factor-κB activation reduces cortical tubulointerstitial injury in proteinuric rats. *Kidney Int* 56:118–134, 1999
9. Donadelli R, Abbate M, Zanchi C, *et al*: Protein traffic activates NF-κB gene signaling and promotes MCP-1-dependent interstitial inflammation. *Am J Kidney Dis* 36:1226–1241, 2000
10. Gomez-Garre D, Largo R, Tejera N, *et al*: Activation of NF-κB in tubular epithelial cells of rats with intense proteinuria–Role of angiotensin II and endothelin-1. *Hypertension* 37:1171–1178, 2001
11. Mezzano SA, Barria M, Droguett MA, *et al*: Tubular NF-κB and AP-1 activation in human proteinuric renal disease. *Kidney Int* 60:1366–1377, 2001
12. Yamamoto Y, Gaynor RB: Therapeutic potential of inhibition of the NF-κB pathway in the treatment of inflammation and cancer. *J Clin Invest* 107:135–142, 2001
13. Sha WC, Liou HC, Tuomanen EI, Baltimore D: Targeted disruption of the p50 subunit of NF-κB leads to multifocal defects in immune responses. *Cell* 80:321–330, 1995
14. Ouaaz F, Li M, Beg AA: A critical role for the RelA subunit of nuclear factor κB in regulation of multiple immune-response genes and in Fas-induced cell death. *J Exp Med* 189:999–1004, 1999
15. Brown K, Gerstberger S, Carlson L, *et al*: Control of IκB-α proteolysis by site-specific, signal-induced phosphorylation. *Science* 267:1485–1488, 1995
16. Hirahashi J, Takayanagi A, Hishikawa K, *et al*: Overexpression of truncated IκBα potentiates TNF-α-induced apoptosis in mesangial cells. *Kidney Int* 57:959–968, 2000
17. Obara H, Takayanagi A, Hirahashi J, *et al*: Overexpression of truncated IκBα induces TNF-α-dependent apoptosis in human vascular smooth muscle cells. *Arterioscler Thromb Vasc Biol* 20:2198–2204, 2000
18. Eddy AA: Interstitial nephritis induced by protein-overload proteinuria. *Am J Pathol* 135:719–733, 1989
19. Barnes PJ, Larin M: Mechanisms of disease: Nuclear factor-κB - A pivotal transcription factor in chronic inflammatory diseases. *N Engl J Med* 336:1066–1071, 1997
20. Moullier P, Friedlander G, Calise D, *et al*: Adenoviral-mediated gene transfer to renal tubular cells in vivo. *Kidney Int* 45:1220–1225, 1994
21. Sumitomo M, Tachibana M, Ozu C, *et al*: Induction of apoptosis of cytokine-producing bladder cancer cells by adenovirus-mediated IκBα overexpression. *Hum Gene Ther* 10:37–47, 1999
22. Miyake S, Makimura M, Kanegae Y, *et al*: Efficient generation of recombinant adenoviruses using adenovirus DNA-terminal protein complex and a cosmid bearing the full-length virus genome. *Proc Natl Acad Sci USA* 93:1320–1324, 1996
23. Kanegae Y, Makimura M, Saito I: A simple and efficient method for purification of infectious recombinant adenovirus. *Jpn J Med Sci Biol* 47:157–166, 1994
24. Kanegae Y, Lee G, Sato Y, *et al*: Efficient gene activation in mammalian cells by using recombinant adenovirus expressing site-specific Cre recombinase. *Nucleic Acids Res* 23:3816–3821, 1995
25. El Nahas AM, Bassett AH, Cope GH, Le Carpentier JE: Role of growth hormone in the development of experimental renal scarring. *Kidney Int* 40:29–34, 1991
26. Johnson TS, Griffin M, Thomas GL, *et al*: The role of transglutaminase in the rat subtotal nephrectomy model of renal fibrosis. *J Clin Invest* 99:2950–2960, 1997
27. Okada H, Moriwaki K, Kalluri R, *et al*: Inhibition of monocyte chemoattractant protein-1 expression in tubular epithelium attenuates tubulointerstitial alteration in rat Goodpasture syndrome. *Kidney Int* 57:927–936, 2000
28. Largo R, Gomez-Garre D, Soto K, *et al*: Angiotensin-converting

enzyme is upregulated in the proximal tubules of rats with intense proteinuria. *Hypertension* 33:732–739, 1999
29. SCHAIER M, LEHRKE I, SCHADE K, *et al*: Isotretinoin alleviates renal damage in rat chronic glomerulonephritis. *Kidney Int* 60:2222–2234, 2001
30. KLIEM V, JOHNSON RJ, ALPERS CE, *et al*: Mechanisms involved in the pathogenesis of tubulointerstitial fibrosis in 5/6-nephrectomized rats. *Kidney Int* 49:666–678, 1996
31. BARONI EA, COSTA RS, VOLPINI R, COIMBRA TM: Sodium bicarbonate treatment reduces renal injury, renal production of transforming growth factor-β, and urinary transforming growth factor-β excretion in rats with doxorubicin-induced nephropathy. *Am J Kidney Dis* 34:328–337, 1999
32. LIU SF, YE X, MALIK AB: In vivo inhibition of nuclear factor-κB activation prevents inducible nitric oxide synthase expression and systemic hypotension in a rat model of septic shock. *J Immunol* 159:3976–3983, 1997
33. BRADFORD MM: A rapid and sensitive method for the quantitation of microgram quantities of protein utilizing the principle of protein-dye binding. *Anal Biochem* 72:248–254, 1976
34. LANE D, PRENTKI P, CHANDLER M: Use of gel retardation to analyze protein-nucleic acid interactions. *Microbiol Rev* 56:509–528, 1992
35. BOHRER H, QIU F, ZIMMERMANN T, *et al*: Role of NFκB in the mortality of sepsis. *J Clin Invest* 100:972–985, 1997
36. ZHU G, NICOLSON AG, COWLEY BD, *et al*: In vivo adenovirus-mediated gene transfer into normal and cystic rat kidneys. *Gene Ther* 3:298–304, 1996
37. CHETBOUL V, KLONJKOWSKI B, LEFEBVRE HP, *et al*: Short-term efficiency and safety of gene delivery into canine kidneys. *Nephrol Dial Transplant* 16:608–614, 2001
38. HEIKKILA P, PARPALA T, LUKKARINEN O, *et al*: Adenovirus-mediated gene transfer into kidney glomeruli using an ex vivo and in vivo kidney perfusion system - First steps towards gene therapy of Alport syndrome. *Gene Ther* 3:21–27, 1996
39. TU Z, KELLEY VR, COLLINS T, LEE FS: I κB kinase is critical for TNF-α-induced VCAM1 gene expression in renal tubular epithelial cells. *J Immunol* 166:6839–6846, 2001
40. SCHLEGEL PG, VAYSBURD M, CHEN Y, *et al*: Inhibition of T cell costimulation by VCAM-1 prevents murine graft-versus-host disease across minor histocompatibility barriers. *J Immunol* 155:3856–3865, 1995
41. SOLEZ K, RACUSEN LC, ABDULKAREEM F, *et al*: Adhesion molecules and rejection of renal allografts. *Kidney Int* 51:1476–1480, 1997
42. ROY-CHAUDHURY P, WU B, KING G, *et al*: Adhesion molecule interactions in human glomerulonephritis: Importance of the tubulointerstitium. *Kidney Int* 49:127–134, 1996
43. RUIZ-ORTEGA M, EGIDO J: Angiotensin II modulates cell growth-related events and synthesis of matrix proteins in renal interstitial fibroblasts. *Kidney Int* 52:1497–1510, 1997
44. GUIJARRO C, EGIDO J: Transcription factor-κB (NF-κB) and renal disease. *Kidney Int* 59:415–424, 2001
45. DENEKE SM, FANBURG BL: Regulation of cellular glutathione. *Am J Physiol* 257:L163–L173, 1989
46. WILD AC, MULCAHY RT: Pyrrolidine dithiocarbamate up-regulates the expression of the genes encoding the catalytic and regulatory subunits of gamma-glutamylcysteine synthetase and increases intracellular glutathione levels. *Biochem J* 338:659–665, 1999
47. VERHAEGH GW, RICHARD MJ, HAINAUT P: Regulation of p53 by metal ions and by antioxidants: Dithiocarbamate down-regulates p53 DNA-binding activity by increasing the intracellular level of copper. *Mol Cell Biol* 17:5699–5706, 1997

Kidney International, Vol. 63 (2003), pp. 936–946

Shedding of growth-suppressive gangliosides from glomerular mesangial cells undergoing apoptosis

Nobuo Tsuboi, Yasunori Utsunomiya, Tetsuya Kawamura, Tetsuro Kikuchi, Tatsuo Hosoya, Tsuneya Ohno, and Hisashi Yamada

Division of Kidney and Hypertension, Department of Internal Medicine, Department of Molecular Genetics and Oncology, Institute of DNA Medicine, Jikei University School of Medicine, Minato-Ku, Tokyo, Japan

Shedding of growth-suppressive gangliosides from glomerular mesangial cells undergoing apoptosis.

Background. Apoptosis of glomerular mesangial cells is a common feature in several types of glomerular diseases. However, its pathophysiologic significance is not known. We recently identified gangliosides as a major growth-inhibitory substance in the conditioned medium of mesangial cells. In this report, we tested whether biologically distinct forms of cell fate, apoptosis and necrosis, could modulate ganglioside shedding from mesangial cells.

Methods. Mesangial cells were exposed to low (10 to 40 mJ/cm^2) and high (400 mJ/cm^2) doses of ultraviolet light to induce apoptosis and necrosis, respectively. Conditioned media were collected and examined for its growth-inhibitory activity for mesangial cells. Ganglioside shedding was analyzed using metabolic labeling and thin-layer chromatography (TLC).

Results. Shedding of gangliosides as well as growth-inhibitory activity in the conditioned medium predominantly increased when mesangial cells were undergoing apoptosis in contrast to that of viable or necrotic mesangial cells. The inhibitory substance in the conditioned medium from apoptotic mesangial cells completely fulfilled the characteristic criteria of gangliosides. This substance was less than 3 kD and was sensitive to neuraminidase digestion. Shedding of gangliosides from mesangial cells reduced significantly when apoptosis was inhibited by overexpression of antiapoptotic gene, *Bcl-XL*. In addition, ganglioside shedding also increased when mesangial cells were exposed to other inducers of apoptosis for mesangial cells (i.e., H_2O_2 and staurosporin).

Conclusion. These results provide the novel link between masangial cell apoptosis and increased release of gangliosides that potentially suppress mesangial cell proliferation and thus indicate a mechanism for the negative regulation of mesangial cell growth by apoptosis.

In the renal glomerulus, apoptosis of resident mesangial cells is observed in several types of human glomerular diseases [1–4]. The pathophysiologic significance of apoptosis in these cells has not yet been determined, but several possibilities have been postulated. Some studies have implicated apoptosis as the major mechanism mediating spontaneous resolution of mesangial hypercellularity in experimentally induced mesangial proliferative glomerulonephritis [5, 6], whereas others have suggested that its inappropriate activation leads to hypocellular scarring, glomerulosclerosis [7, 8]. These data emphasize that the outcome of glomerular diseases is most unlikely to be determined solely by the regulation of resident cell division. Rather, it appears that a crucial factor is the balance between cell proliferation and cell death by apoptosis [9].

Accumulating data indicate that there are likely to be many counterbalancing influences on whether cells divide or die. For example, many potent regulators of mitogenesis, cytokines, peptide growth factors [10], and extracellular matrices [11], also alter susceptibility to apoptotic stimuli in mesangial cells. In addition, it has been suggested in other cells that apoptosis is controlled by certain growth-related signal transducers [12, 13] and cell-cycle molecules [14, 15]. However, besides intense effort for mechanisms involved in the regulation of proliferation and apoptosis, it is largely unknown how these different processes are coordinated during restoration of injured tissues, including inflamed glomeruli.

Gangliosides are neuraminic acid–containing glycosphingolipids that are constituents of the plasma membranes of various cells [16]. These molecules are synthesized by a stepwise addition of sugar residues to the glycan side chain of ceramide backbone by specific enzymes [16]. Gangliosides are often shed from the cell membrane into the extracellular microenvironment and play important biologic roles in certain pathologic situations. For example, some tumor-derived gangliosides show immunosuppressive effects [17, 18], while others have angiogenic properties [19, 20]. Recently, we demonstrated that conditioned medium of cultured rat glomerular mesangial cells exhibited extremely powerful growth-inhibi-

Key words: mesangial cell, apoptosis, ganglioside.

Received for publication June 21, 2002
and in revised form September 27, 2002
Accepted for publication October 16, 2002